# Long-term culture system for deep-sea mussels *Gigantidas childressi*

**Claas Hiebenthal** [ORCID],[1]* **Finn-Ole Gehlert** [ORCID],[2] **Mark Schmidt** [ORCID],[1] **Thorsten B. H. Reusch** [ORCID],[1,2] **Frank Melzner** [ORCID][1,2]
[1]GEOMAR Helmholtz Centre for Ocean Research Kiel, Kiel, Germany
[2]Christian-Albrechts-Universität, Kiel, Germany

## Abstract

The simulation of deep-sea conditions in laboratories is technically challenging but necessary for experiments that aim at a deeper understanding of physiological mechanisms or host-symbiont interactions of deep-sea organisms. In a proof-of-concept study, we designed a recirculating system for long-term culture (>2 yr) of deep-sea mussels *Gigantidas childressi* (previously *Bathymodiolus childressi*). Mussels were automatically (and safely) supplied with a maximum stable level of ~60 $\mu$mol L$^{-1}$ methane in seawater using a novel methane–air mixing system. Experimental animals also received daily doses of live microalgae. Condition indices of cultured *G. childressi* remained high over the years, and low shell growth rates could be detected, too, which is indicative of positive energy budgets. Using stable isotope data, we demonstrate that *G. childressi* in our culture system gained energy, both, from the digestion of methane-oxidizing endosymbionts and from digesting particulate food (microalgae). Limitations of the system, as well as opportunities for future experimental approaches involving deep-sea mussels, are discussed.

Most pelagic and benthic deep-sea food webs depend on limited amounts of organic material that originates in the euphotic zone and sinks to the deeper ocean (Billett et al. 1983; Gage 2003). As a result, the biomass of most deep-sea species assemblages is low (Sanders and Hessler 1969). However, chemosynthetic deep-sea habitats such as "hot vents" or "cold seeps" can host a set of specialized organisms thriving at high abundances with biomasses of up to 30 kg m$^{-2}$ (e.g., Paull et al. 1984; Sibuet and Olu 1998). At "cold seep" sites, cool and often high-saline sea water seeps from the sea floor (e.g., 120 g kg$^{-1}$ and 6.5–7.2°C at Brine-Pool-NR-1, Northern Gulf of Mexico; e.g., Smith et al. 2000; Berger and Young 2006). The seeping water is usually highly enriched in reduced compounds, such as hydrogen sulfide or methane (e.g., Tunnicliffe et al. 2003; Bergquist et al. 2005), that serve as main energy sources for the organisms dwelling in such chemosynthetic ecosystems. Thus, these systems do not rely on solar energy for carbon fixation (Tunnicliffe et al. 2003). Thiotrophic, methylotrophic, or methanotrophic microorganisms use chemical energy via oxidation and fixation of the reduced inorganic molecules from the seep water (McCollom

and Shock 1997; Duperron et al. 2007). Some of these form bacterial mats on the sea floor, which grazers like shrimp or snails feed upon (Dattagupta et al. 2007). Other chemolithoautotrophic bacteria developed close symbiotic relationships with metazoans, such as polychaete worms, sponges, or bivalve molluscs (MacDonald et al. 1990; Tunnicliffe et al. 2003; Cordes et al. 2009; Nishijima et al. 2010). These symbionts allow their animal hosts to indirectly obtain energy from inorganic molecules dissolved in the seawater, either by translocation of fixed carbon products to the host ("milking type") or by digestion of the bacteria by their hosts ("farming-type" carbon transfer; Streams et al. 1997).

The deep-sea mytilid mussel *Gigantidas childressi* (subfamily Bathymodiolinae, family Mytilidae; originally described as "*Bathymodiolus*" *childressi* [Childress et al. 1986; Gustafson et al. 1998]) occurs in high abundances at cold seeps from about 550 to more than 2200 m depth on the upper as well as the lower continental shelf in the Gulf of Mexico (Nix et al. 1995; Gustafson et al. 1998; Faure et al. 2015). The mussel holobiont can utilize methane as its only energy and carbon source (Cary et al. 1988). Metanotroph γ-proteobacteria that employ a ribulose-monophosphate pathway to fix carbon ("type 1 methanotrophs") are concentrated in vacuoles of symbiont-containing bacteriocytes in the outer (water-facing) gill epithelium of mussels of the Bathymodiolinae subfamily (Fiala-Médioni et al. 1986; Duperron et al. 2007; Wentrup et al. 2014). The mussels generate a ciliary-driven water current to lead methane-rich water past their gills, where methane can diffuse into the gill tissue to supply the demands of the symbionts. The methanotrophic bacteria proliferate and are

*Correspondence: chiebenthal@geomar.de

eventually digested by their hosts ("farming-type" carbon transfer; Fisher and Childress 1992; Streams et al. 1997). However, bathymodioline mussels do not always solely depend on the carbon fixation of bacterial symbionts (Riou et al. 2010). While the host's gastrointestinal tract is often largely reduced in other symbiotic holobionts, this is not the case in *G. childressi*. Even though recent findings show that the digestive system of bathmodiolins indeed undergoes a drastic structural reduction during metamorphosis from the photo-heterotrophic living planktonic larvae to the sessile mussels (Franke et al. 2021), the adult animals can still filter and digest particulate organic matter (POM) from the water column (Cary et al. 1988; Page et al. 1990; Pile and Young 1999). At low methane availability, bathymodioline mussels may even obtain the majority of the assimilated carbon from POM (Martins et al. 2008; Riou et al. 2010).

Experimental work with living deep-sea animals is extremely challenging. As it is very time-consuming and costly to reach deep-sea mussel reefs via remotely operated vehicles, in situ manipulations—such as transplantation experiments—are rare (Nix et al. 1995; Ravaux et al. 2019). Some experiments could be conducted on board the research vessel right after collecting deep-sea mussels (e.g., Pile and Young 1999), but many deep-sea animals rapidly die when taken to the surface. Furthermore, it is technically challenging to recreate deep-sea pressure and water chemistry in laboratories, which makes in vitro experiments very difficult and often only possible for short-term applications (e.g., Young et al. 1995; Hourdez 2018; Huang et al. 2019; Mitchell et al. 2020). This is primarily due to the difficulty of incorporating nitrification-biofilters into pressurized systems that could remove accumulating and ultimately toxic ammonia (Koyama et al. 2002; Shillito et al. 2015). Longer-term laboratory experiments, however, are crucial to understand, for example, energy metabolism at varying seawater methane concentrations, the relative importance of energy uptake via autotroph symbionts vs. filtration of POM, as well as the physiological mechanisms underlying host-symbiont energy transfer. Ultimately, experimental culturing systems that can simulate realistic seep environments could enable us to also study reproductive processes and larval development, behavior, and chemotaxis—important aspects of bathymodioline mussel biology that will allow us to better constrain larval drift models, population connectivity, and ultimately, guide deep-sea conservation efforts (Breusing et al. 2016; Franke et al. 2021).

Here, we describe a recirculating culturing system that allowed us to cultivate deep-sea mussels *G. childressi* for multiple years while supplying them with constant methane levels as well as POM (microalgae). We demonstrate that cultured mussels maintain and increase the ability to consume methane and are able to invest surplus energy into shell thickness growth. Tissue C and N stable isotope data reflect a mixed diet of autotrophic symbionts and POM. We discuss the

limitations of the culturing system as well as implications for future culture systems for deep-sea organisms.

## Materials and procedures

### Mussels and sampling sites

We cultured two batches of *G. childressi* specimens for altogether 36 and 27 months, respectively. The deep-sea mussels of the first batch (208 specimens, "batch 1") were collected by E/V "Nautilus" using the ROV "Hercules" southwest of New Orleans in the Gulf of Mexico at station GC233 ("Brine Pool NR-1"; 27°43.4076′N, 91°14.7798′W) on 13 July 2014 at a depth of 650 m. At this site, cold and high-saline water seeps from the ocean floor and—due to the higher density—fills a "brine pool" which is surrounded by a *G. childressi* mussel bed (MacDonald et al. 1990). The mussels arrived at GEOMAR (Kiel, Germany) 14 d after being collected. The second batch of *G. childressi* (35 specimens, "batch 2") was collected by MSV "Ocean Intervention II" using the ROV "Global Explorer" northeast of the first site at station GC249 (27°43.7274′N, 90°31.0140′W) in 811 m depth on 18 June 2017.

The mussels were transported within 4 d by ship and truck to the Fisher deep-sea lab at Pennsylvania State University, State College, PA. Here, the experimental animals were cultured in a recirculating seawater aquarium system ($T = 8°C$, $S = 34$) that continuously received methane-saturated seawater. Seawater methane concentrations were not quantified during this time period. Subsequently, after 2 months, animals were shipped by plane in cooled jars ($T = 5$–$8°C$, $S = 34$) to GEOMAR (travel time < 24 h). There was no mortality during the transport of both batches.

### Description of the *G. childressi* culture system

The long-term deep-sea mussel culture system at GEOMAR that enabled continuous culture from July 2014 to November 2019 is located in a constant temperature room and is based on a classical recirculating aquarium system (Fig. 1). The system consists of three 25 L glass culture tanks ("2") that receive water via gravity feed from a 25 L header tank ("1") at a constant flow rate of 150 mL min$^{-1}$. All tanks are covered with acrylic glass lids (not gas-tight because the pressurized air supply would otherwise impede the gravity-feed water flow), and there are headspaces between the water surface and these lids (4 cm in the 25 L tanks and 10 cm in the filter sump). Water leaving the culture tanks via overflow pipes (PVC) is collected in a 100 L filter sump ("3"), where it is processed by a nitrification filter ("4", pond external filter type 3455, EHEIM, Deizisau, Germany, filled with 12 L of HDPE bio carriers), as well as by a protein skimmer ("6", ACF 1000 V, AquaCare GmbH & Co. KG). Subsequently, the culture water is led by a UV lamp ("7", hw UV-water sterilizer Model 500, Wiegandt GmbH) before being pumped back to the header tank. During the 5.5 yr of culture, the water temperature was kept constant at $7.9 \pm 0.2°C$ and pH (NBS scale) was $8 \pm 0.1$. Ammonia and nitrite concentrations were assessed biweekly and
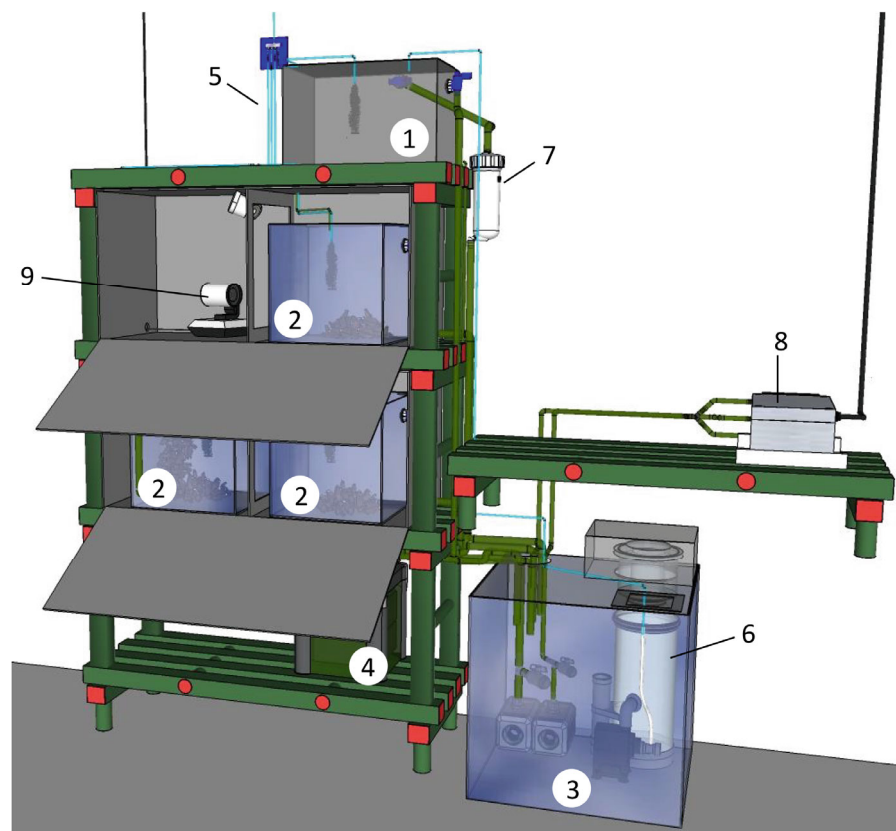
**Fig. 1.** 3D sketch of the 200 L water recirculating culture system to maintain deep-sea mussels *Gigantidas childressi*. Details: (1) header tank, (2) culture aquariums with deep-sea mussels, (3) filter sump, (4) biofilter, (5) gas supply line with air–methane mixture, (6) protein skimmer, (7) UV-sterilizer, (8) methane sensor, (9) IR camera. (1), (2), and (3) are covered with transparent acrylic glass lids.

concentrations were always <0.05 mg L$^{-1}$. Thirty percent of the system water was exchanged each week. The culture water was mixed from sand-filtered Baltic Sea water (salinity 12–20, GEO-MAR central facility) from Kiel Fjord and a commercial sea salt mixture (Pro Reef, Tropic Marin AG). Salinity was set to 34.5.

As *G. childressi* is sensitive to mechanical disturbances, we placed the culture tanks on rubber mats and in two PVC boxes with openings for water and gas lines as well as flap doors at the front to access the tanks. The boxes also allowed for culturing the mussels almost full time in complete darkness, only interrupted by short daily check-ups of the system and occasional cleaning of the aquaria. An IR camera was installed to be able to observe the mussels (Fig. 1: "9").

**Methane supply**

Central to our culture system is a methane–air gas mixing device that is placed in a room next door to the deep-sea mussel culture facility. This mixing device continuously enriches the pressurized air ("natural" air, continuously provided by a central supply system) led to the culture system with methane (Fig. 2). The gas mixing device consists of a thermal gas flow sensor ("red-y smart meter," 5–500 L h$^{-1}$, Voegtlin Instruments) and a thermal gas flow controller ("red-y smart controller,"

0.2–20 L h$^{-1}$, Voegtlin Instruments) that injects pure methane from a gas tank into the airflow, the amount depending on the flow rate and the desired methane level. A custom-made control unit (HTK Hamburg GmbH) processes the airflow rate signal from the flow sensor and defines the methane flow rate via the flow controller. Desired methane levels (0.0–4.0% methane in the air) can be set using software (EasyHTK, HTK) on a USB-connected PC. The gas mixture flow rate can be adjusted via a flowmeter (Q-Flow V100-140, Voegtlin Instruments).

The gas mixture is then led in a gas-tight polyurethane line (PUR C 98A) from the gas mixing device room to the *G. childressi* culture system room. Both, the header tank and the three culture tanks of the culture system are equilibrated with the gas mixture using diffusor stones at ~1.7 L gas mixture min$^{-1}$ (Fig. 1: "5"). Also, the protein skimmer is supplied with the methane–air gas mixture instead of the methane-poor culture room air. The total gas flux of the 4% methane–air mixture to the recirculation culture system is 400 L h$^{-1}$.

**Feeding with microalgae**

Apart from the consumption of methanotrophic symbionts, *G. childressi* can obtain energy from filtered organic particles as well (Cary et al. 1988; Page et al. 1990; Pile and
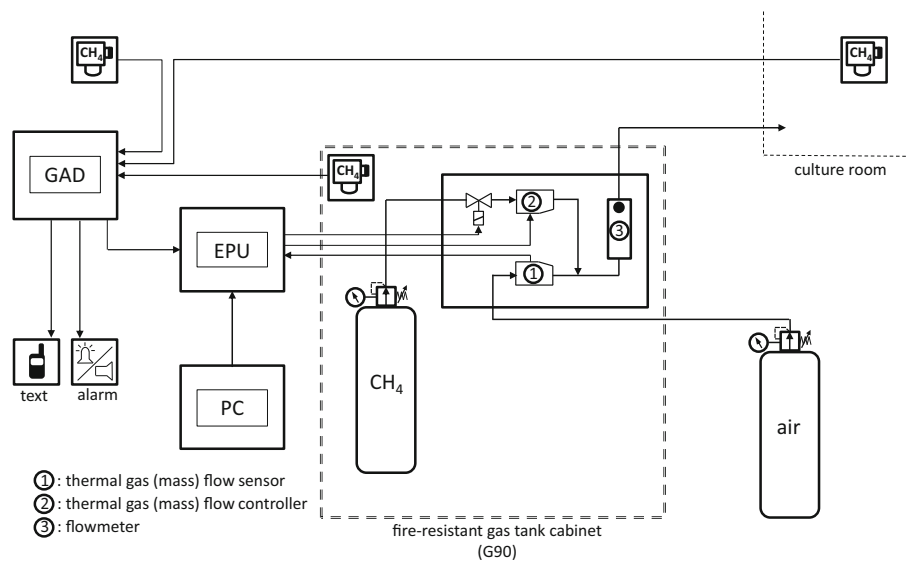
**Fig. 2.** Technical sketch of the gas mixing device. The airflow is measured by the flow sensor (1) and an evaluating processor unit (EPU) controls how much methane is injected by the flow controller (2). Methane–air mixture flow can be controlled by a flowmeter (3). A gas alarm device (GAD) receives methane level signals from three sensors (in the fire-resistant gas tank cabinet, in the gas mixture room and in the deep-sea mussel culture room) and triggers alarm signaling, text messaging and closing of the magnetic valve (cutting-off methane flow) when alarm levels are reached.

Young 1999; Bettencourt et al. 2011). Thus, our deep-sea mussels were also fed 5 d a week with 450 mL *Rhodomonas* sp. microalgae stock solution (with $\sim 2 \times 10^6$ cells mL$^{-1}$, corresponding to $\sim 4500$ cells mL$^{-1}$ after being diluted in the 200 L culture system, or $\sim 4.3 \times 10^6$ cells mussel$^{-1}$). This cryptophyte is very rich in polyunsaturated fatty acids (Renaud et al. 1999), is regularly used as food in experiments with shallow water mytilids (e.g., Thomsen et al. 2010; Riisgård et al. 2011, 2012), and is permanently cultured at GEOMAR as nutritious food for filter feeding organisms in artificial seawater supplied with "Walne's medium" including macronutrients, vitamins and trace elements (Walne 1970).

**Safety measures**

As our deep-sea mussel culturing system can be run close to the lower explosion limit for methane in the air, a set of safety measures was installed to exclude the formation of an explosive atmosphere in a non-explosion-safe environment:

i. The maximum methane level that can be produced by the gas mixing device is (software-wise) restricted to 4%, which is below the explosion limit of 4.4% methane in the air.
ii. The gas tank, as well as the mixing device's gas leading parts (flow sensor, flow controller, flowmeter), are placed inside a fire-resistant gas tank cabinet (G90, in accordance with EN 14470-2, fire resistance of 90 min). Only the processor unit is placed outside, and only the gas mixture with a maximum of 4% methane leaves the cabinet in gas-safe lines (no pure methane).

iii. Methane sensors are placed in the constant temperature room (*G. childressi* culture room), in the gas mixing room, and in the fire-resistant gas tank cabinet containing the mixing device. A central gas alarm device raises the alarm when two alarm levels are reached: *alarm level 1* at 0.88% methane (20% of lower explosion limit, flashlight) and *alarm level 2* at 1.76% methane (40% of lower explosion limit, flashlight, and alarm sound). At both alarm levels text messages are sent to operating personnel.
iv. At *alarm level 1* a magnetic valve between the gas bottle and flow controller is closed and, hence, the methane flow is interrupted.
v. Power failure also causes the magnetic valve to close, and the alarm device to send a text message to operating personnel.
vi. Operating personnel controls methane consumption rates of the mixing device and methane concentration in the culture system water daily to detect potential leaks.

Costs for setting up the entire deep-sea mussel culture system installed in 2013–2014 were $\sim$€17,000 for the culturing system (including methane-sensing instrument HydroC® CH$_4$ FT), another $\sim$€17,000 for the gas mixing system, and €7000 for the gas safety surveillance system. Not included are repeatedly occurring costs for maintenance and methane consumption (at 400 L h$^{-1}$ production of 4% methane–air mixture: $\sim$10,000 L methane, corresponding to one 50 L 200 bar cylinder month$^{-1}$). We used technical grade methane with a purity level of 99.5% which is well in the range of the methane portion of natural gas at Gulf of Mexico seeps (e.g., 98.05–99.98%; Bernard et al. 1976).

## Assessment

### System performance: Metrics

#### Performance of methane supply

To monitor the performance of the methane supply system, methane concentrations in the culture seawater were continuously measured by a flow-through instrument that can determine seawater methane concentration with an accuracy of $\pm 0.1\ \mu\mathrm{mol\ L}^{-1}$ (CONTROS HydroC® CH$_4$ FT, 4H-JENA engineering). The HydroC® is placed above the culture system's filter sump (Fig. 1: "8"). Culture seawater is continuously pumped from the filter sump via a PVC pipe to the methane sensor (and back) at a rate of 2 L min$^{-1}$ (EHEIM universal pump 1200, EHEIM).

#### Mussel condition and growth

Two sets of experiments were conducted during the culture system development process. In the first set, *G. childressi* from batch 1 were cultured with a continuous supply of 20–30 $\mu$mol L$^{-1}$ methane in seawater, as well as with daily additions of microalgae *Rhodomonas* sp. (resulting in 4500 cells mL$^{-1}$ in the culture seawater) to obtain first insights into the mussels' energy uptake. Based on findings from this culture period, we decided to increase the seawater methane concentration, and to conduct a second set of experiments with 35 mussels from batch 2 under three different nutritional regimes: (1) exclusively methane addition (60–70 $\mu$mol L$^{-1}$) = "m", (2) methane (60–70 $\mu$mol L$^{-1}$) and microalgae (*Rhodomonas* sp.) addition = "a + m", and (3) exclusively microalgae (*Rhodomonas* sp.) addition = "a." To achieve nutrition treatment "a" one of the 25 L culture aquaria was separated from the main culturing system and the mussels exclusively fed with *Rhodomonas* sp.: twice a day, 125 mL of *Rhodomonas* sp. stock solution was poured directly into the aquarium resulting in ca. 10,000 cells mL$^{-1}$ ($\sim$21 $\times$ 10$^6$ cells mussel$^{-1}$) after being diluted in the 25 L of seawater. The water of this aquarium was treated with a separate nitrification filter (ecco pro 200, EHEIM) and protein skimmer (Power Skimmer WT350, Sander) placed in an extra 25 L filter sump. The *G. childressi* in one of the aquaria of the main system continued to receive methane and *Rhodomonas* sp.: again, twice a day, 125 mL stock solution was poured directly into the 25 L aquarium resulting in 10,000 cells mL$^{-1}$ ($\sim$21 $\times$ 10$^6$ cells mussel$^{-1}$) after being diluted in culture seawater. In the remaining ("m")-aquarium, phytoplankton addition was stopped. The three-step filtering of seawater in the main recirculation system (by nitrification filter, protein skimmer and UV-clearer) prevented unconsumed microalgae from being transported to the "m"-treatment aquarium. This second set of experiments aimed at a deeper understanding of *G. childressi* energy acquisition modes (Table 1). At the end of November 2019, all remaining specimens were sacrificed for final measurements.

Condition of cultured deep-sea mussels: To measure the general condition of cultured *G. childressi*, the condition index ($C_i$) was used as the quotient of ash-free dry weight (AFDW) and inner mussel shell volume (Smith 1985; Davenport and Chen 1987; Smith et al. 2000, Eq. 1).

$$\text{condition index}\ \left(\mathrm{g\,mL}^{-1}\right) = \frac{\text{ash} - \text{free dry weight (g)}}{\text{shell volume (mL)}}. \qquad (1)$$

To assess the $C_i$, the mussels' soft tissue was removed from the shells, dried for 24 h at 80°C and the dry weight was measured. Subsequently, the tissue was incinerated at 500°C to measure the ash weight which was subtracted from the dry weight to obtain AFDW.

The inner shell volume was measured indirectly via the weight of fine silica sand (grading 50–1000 $\mu$m) that filled the shell: The mussel shells were filled with water to ensure a balanced position and glued to glass slides. After drying, the shells were weighed with and without sand. A calibration curve produced using 1–40 units of a standardized cup of exactly 0.2602 mL (Supporting Information Fig. S2) allowed us to estimate shell volume from the sand's weight (Eq. 2):

$$\text{shell volume (mL)} = \text{sand mass (g)} \times 0.7728\ \left(\mathrm{mL\,g}^{-1}\right). \qquad (2)$$

$R^2 = 0.99$, $n = 32$, sand volume range 0.26–10.41 mL.

Shell lengths of the sacrificed *G. childressi* were also measured to correlate the mussels' condition with their size. $C_i$s of subsamples of cultured deep-sea mussels were assessed three times: once with mussels of batch 1 (12 specimens in August 2016), twice with mussel of batch 2 (3 specimens in August 2017, 12 specimens in November 2019, Table 1).

Growth of cultured deep-sea mussels: Shortly after the start of the *G. childressi* culture efforts with mussel batch 1 on 11 September 2014, the animals were stained with the fluorescent dye calcein (Sigma C0875). Calcein can be excited at 488 nm and emitted at 515 nm and is rapidly incorporated into the shell of molluscs (Holcomb et al. 2013; Ramesh et al. 2017). Hence, shell length and thickness growth rates can be followed using a fluorescence stereo microscope (Nedoncelle et al. 2013). Calcein was added to the culture system (50 mg L$^{-1}$) and subsequently—over the course of 2 months—diluted via regular water changes, allowing the mussels to incorporate the dye into newly grown shell material. In August 2016, 12 *G. childressi* individuals were sacrificed to analyze the growth of calcein-stained animals. Shells were analyzed using a Leica M165 FC stereo microscope at magnifications between 40- and 120-fold using a GFP filter set (excitation: BP 450–490 nm, emission: LP 515 nm) and EL6000 light source (Leica Camera AG). Shells were first analyzed for longitudinal growth, then manually broken along the length axis and imaged in cross-section at the leading edge (*see* Fig. 3). Images were analyzed using Leica LAS X software. To follow *G. childressi* growth rates macroscopically as well, all mussel shells were also scraped with a rotary tool to remove the periostracum at the outer shell margin. The distance measured from these markings to the margin of newly grown shell

**Table 1.** Overview of *Gigantidas childressi* experiments with mussels from batches 1 and 2. Numbers in parenthesis indicate months in GEOMAR deep-sea culture facility after which the respective experiment was conducted.

| | | Experiment 1 (batch 1) | Experiment 2 (batch 2) |
|---|---|---|---|
| Site of origin | | Brine Pool 650 m depth: 27°43.4076′N, 91°14.7798′W | GC249, 811 m depth: 27°43.7274′N, 90°31.0140′W |
| Date of collection | | July 2014 | June 2017 |
| Start of culture at GEOMAR | | 14 d after collection | August 2017* |
| Total time in GEOMAR fascility | | 36 months | 27 months |
| Nutritional conditions during culture | | 20–30 $\mu$mol L$^{-1}$ CH$_4$ + | "m": 60–70 $\mu$mol L$^{-1}$ CH$_4$ |
| (= acclimation phase)† | | *Rhodomonas* | "a + m": 60–70 $\mu$mol L$^{-1}$ CH$_4$ + *Rhodomonas* |
| | | | "a": *Rhodomonas* |
| Experiments/analyses conducted | | | |
| Calcein staining | | September 2014 (2) | – |
| Condition index ($C_i$) | | June 2016 (23) | August 2017 (0) |
| | | | November 2019 (27) |
| Shell growth | | June 2016 (23) | November 2019 (27) |
| CH$_4$ and O$_2$ consumption | | December 2015 (17) | December 2017 (3.5) |
| (Only) CH$_4$ consumption | | | July 2019 (23) |
| Activity vs. [CH$_4$] | | | November 2019 (15) |
| Microalgae consumption | *Rhodomonas* sp. | August 2016 (25) | April 2018 (8) |
| | *Nannochloropsis* sp. | August 2016 (25) | |
| Stable isotopes | | | November 2019 (27) |
| Final sampling | | | November 2019 (27) |

*Two months in Fisher's deep-sea lab.
†Increased methane supply and nutrition treatments started at the start of the batch 2 mussel culture.

material then served as a measurement of shell growth. The shells of batch 2 mussels were only marked with these scrapings (no calcein staining).

### Methane and oxygen consumption of deep-sea mussels

To measure *G. childressi* gas consumption rates, the animals were placed into gas-tight closed respirometer vessels (500 mL glass bottles) that were prepared with oxygen sensor spots
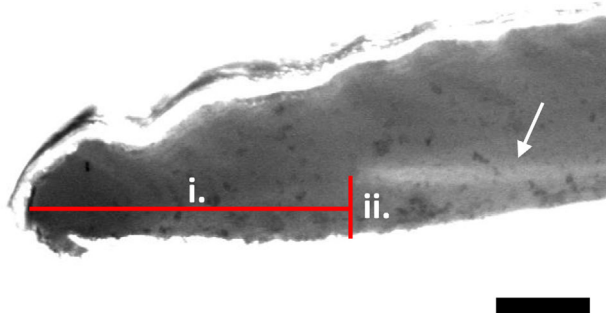


**Fig. 3.** Shell length (i.) and thickness (ii.) growth measurements of cultured *Gigantidas childressi* from batch 1 after 23 months of culture. Calcein-marked growth bands (arrow) imaged with a Leica M165 FC fluorescence stereo microscope. Scale (black bars) = 100 $\mu$m.

(SP-PSt3-NAU, PreSens Regensburg; resolution $\pm0.1\%$ at 20.9% O$_2$ or $\pm0.04$ mg L$^{-1}$ at 9.1 mg L$^{-1}$) to measure oxygen concentrations with a four-channel Oxy-4 micro instrument (PreSens) via optical fibers every 15 min (e.g., Vajedsamiei et al. 2021; Supporting Information Fig. S7). The animals needed some time to recover from being transferred into the respirometers before they opened their valves and started filtering seawater. This recovery time period varied between 1 and 3 h and could be estimated from the point of time when the oxygen concentrations in the respirometers started to decline. Periods of 15–30 min without decreasing oxygen content indicated shell closure and cessation of filtration and gas exchange rates. Mytilids are able to dramatically and rapidly reduce metabolic rates when they close their valves (Supporting Information Fig. S7; e.g., Vajedsamiei et al. 2021). Measurements were stopped after 8 h.

Methane consumption rates were measured as two-point measurements parallel to the respiration measurements using water samples from the respirometers. For this purpose, water samples were taken (in gas-tight 20 mL brown glass bottles) at the beginning and at the end of the measuring period. Gas bubble-free water samples were poisoned immediately after sampling with 100 $\mu$L saturated mercuric chloride solution. During the measurement period, the measuring chambers remained closed and without any gas bubbles. Methane

concentrations were measured later on an HP 5890 gas-phase chromatograph (Hewlett-Packard) using the headspace technique (Bange et al. 2010). During the measurements of batch 1 mussels and the first measurements of batch 2 mussels, the activity of mussels could be estimated from the parallel respiration measurements, *see* above (Supporting Information Fig. S7). During the 2nd measurements of methane consumption of batch 2 mussels, however, the mussels' activity (open vs. closed valves) was individually monitored using cameras (QuickCam®, Logitech, connected via USB to a PC). Thus, we were able to normalize methane consumption to the amount of time animals were active (open valves, high respiration rates).

During each run, one water filled respirometer was used as the control for bacterial oxygen and methane consumption. Bacterial control respiration rates were always < 1% of experimental animal respiration rates. Methane and oxygen consumption rates ($M_{CH4}$ and $M_{O2}$, respectively) per g mussel soft body mass were calculated as the difference of gas concentrations at the start ($C_{start}$) and at the end of the measurement ($C_{end}$), multiplied by the volume of the measuring chamber and followed by subtraction of control (microbial) respiration rates (Eq. 3, "time": sum of time periods with actively filtering mussels):

$$M\left(\mu\text{mol g}^{-1}\text{h}^{-1}\right) = \frac{\{(C_{start} - C_{end}) \times V_{chamber}\} - \{(C_{start\_control} - C_{end\_control}) \times V_{chamber\_control}\}}{\text{soft body mass (g)} \times \text{time (h)}}. \tag{3}$$

The soft tissue mass of the utilized mussels could not be assessed directly as 20–50% of the soft tissue (the gills) were sampled for symbiont density analyses for a different project (publication in prep.). Total soft tissue could not be weighed before gill sampling as this would have corrupted the gill samples. Hence, soft tissue masses were indirectly estimated from a total weight—wet weight relation obtained from mussels sacrificed for $C_i$ analyses (Eq. 4; Supporting Information Fig. S3):

$$\text{Wet weight (g)} = \text{total weight (g)} \times 0.2369, R^2 = 0.976,$$
$$n = 9, \text{shell length range} : 24 – 73 \text{ mm} \tag{4}$$

Methane and oxygen consumption measurements were conducted with both batches of animals at different time periods: animals of batch 1 following culture at 20–30 $\mu$mol L$^{-1}$ methane ($n = 12$) and animals of batch 2 following culture under the three different nutrition regimes: "m," "a + m," and "a" ($n = 3$ each). Furthermore, batch 2 mussels' methane consumption rates (of the same mussel individuals) were measured again after another 19.5 months of exposure to the same nutrition treatments. This

second set of measurements aimed at exploring possible acclimation effects of *G. childressi* or symbionts over time (Table 1).

### G. childressi *gape behavior in relation to water methane concentration*

Repeated IR camera observations of cultured *G. childressi* suggested that the deep-sea mussels react to changes in culture seawater methane concentrations with increased or reduced filtering activity. To test whether these observations can be repeated under controlled conditions, a simple experiment was performed in one of the aquaria: nine batch 2 *G. childressi* individuals from the three treatments were placed into a perforated acrylic glass rack with multiple chambers to constrain animals (Supporting Information Fig. S4). Strong aeration and an additional circulation pump (Koralia, 900, HYDOR srl) increased water movement in the aquarium and into the acrylic glass rack. Mussel filtering behavior was observed with the IR camera while culture system seawater methane concentrations were raised or lowered. During the experimental observations, methane seawater concentration of the whole culture system was raised in five steps from 0 to ~60 $\mu$mol L$^{-1}$ (by daily increasing the methane concentration in the bubbling air by 0.8%), and then, subsequently, reduced stepwise back to 0 $\mu$mol L$^{-1}$ (Supporting Information Fig. S5). Starting in November 2019, this procedure was repeated three times. The IR camera took pictures at a rate of 30 h$^{-1}$. The pictures were analyzed after the experiment was finished by creating time-lapse videos. Videos were observed and periods with opened valves were quantified for each animal. Mussels were assumed to be actively filtering with opened valves. *G. childressi* filtering activity was expressed as minutes of activity per hour.

#### *Particulate food consumption*

To estimate the fraction of energy that can be obtained by the mussels in our culture system through the consumption of POM, we conducted two experiments (Table 1) similar to those published by Page et al. (1990) using microalgae as a food source.

The first experiment aimed at assessing consumption preferences of different-sized mussels when offered two different types of phytoplankton food. We placed six batch 1 *G. childressi* (each three of two size classes: "small": 51 mm $\pm$ 3 SD, "large": 77 mm $\pm$ 4 SD) individually into 500 mL glass bottles filled with seawater and continuously aerated with a 3% methane–air mixture (40–50 $\mu$mol L$^{-1}$) via diffusor stones,

which also ensured mixing of algae within bottles. Two more bottles were used as controls and did not contain animals. Before microalgae were added to the bottles, 1 mL samples were taken to determine background particle concentrations. Microalgae culture concentrations were measured using a flow cytometer (Accuri 6, BD Biosciences). Cell concentrations at the start of the experiments were set to ∼7000 cells mL$^{-1}$ (Foster-Smith [1975]; Page et al. [1990]). Microalgae were allowed to be evenly distributed by the diffusor stone-induced currents in the bottles. Hence, the first samples ($t_0$) were taken after 15 min when mixing was complete. Further samples were taken after 3, 7, 11, and 24 h. At each sampling time point, 1 mL of seawater was taken from each bottle and microalgae cell concentrations were measured on the flow cytometer. The experiment was conducted first with *Rhodomonas* sp. (cell size: 5–8 $\mu$m) and subsequently—2 d later, using the same mussel individuals—with *Nannochloropsis* sp. (cell size: 2–4 $\mu$m) to test for possible feeding preferences of *G. childressi*. Clearance rates ($R_C$) were calculated after Coughlan ([1969]) and Jacobs et al. ([2015]):

$$R_C \left(\mathrm{mL\,h^{-1}}\right) = \frac{V}{t} \times \left\{ \left( \ln \frac{C_0}{C_t} \right) - \left( \ln \frac{C_0'}{C_t'} \right) \right\}, \qquad (5)$$

where "$V$" is the water volume (mL), "$t$" is the time since the start of the experiment (h), "$C_0$" and "$C_t$" are the cell concentrations of bottles with mussels filtering at $t_0$ and $t$, and "$C_0'$" and "$C_t'$" of controls at $t_0$ and $t$, respectively (cells mL$^{-1}$).

The second experiment aimed at measuring the filtering capacities of mussels that were cultured in the three different nutrition treatments ("m," "a + m," and "a"). We used three batch 2 *G. childressi* specimens (all from the same size class: 65 mm ± 3 SD) from each of the three nutritional treatments. The mussels were placed in 500 mL bottles that were equilibrated with a 4% methane–air mixture (corresponding to 60–70 $\mu$mol L$^{-1}$) as described above. Three additional bottles were used as controls. Cell concentrations were measured with a Coulter Counter (Z2 Coulter particle count and size analyzer, Beckman Coulter) which allowed for more rapid data acquisition when compared with the flow cytometer. Microalgae density was set to ∼7000 cells mL$^{-1}$ at the start of the experiments. Samples were taken after 15 min ($t_0$) and after 3, 7, and 11 h. Microalgae consumption rate of *G. childressi* from the "a" treatment group were conducted twice: Once in water equilibrated with 4% methane–air mixture and once in water without methane.

### Stable isotopes

We used batch 2 deep-sea mussel specimens acclimated to all three nutritional regimes (Table [1]) for stable isotope ($\delta^{15}$N, $\delta^{13}$C) analyses. In addition, three specimens of batch 2 were sampled directly when they arrived in our lab ("$t_0$"). The soft tissues of the mussels were frozen at −20°C, stored for 1 week ("$t_0$" samples for 27 months), and subsequently freeze-dried (in a lab freeze dryer Alpha 1-4 LSC, Martin Christ Freeze

Dryers; time: 2–5 d until all water had left the sample, time depending on the tissue volume respectively water content) and ground to powder. *Rhodomonas* sp. culture samples were centrifuged for 15 min at 800 rpm and the supernatant was discarded. The concentrated cell suspension was also frozen at −20°C, freeze-dried, and ground to powder.

Total particulate carbon and nitrogen content and isotopic signatures were analyzed according to Sharp ([1974]). 0.5 mg of each sample was weighed into tin cups. Inorganic carbon was removed by the addition of 0.2 $\mu$L of 10% HCl. After drying the samples, the procedure was repeated once more and the cups were closed and analyzed. The samples were then combusted in a CN analyzer (Flash IRMS EA IsoLink CN Thermo Fisher) connected to a DELTA V Adv MS isotope ratio mass spectrometer (Thermo Fisher Scientific). Isotopic ratios $\delta^{15}$N and $\delta^{13}$C were calculated as:

$$\delta X\,(‰) = \left\{ \left( \frac{R\_\mathrm{sample}}{R\_\mathrm{standard}} \right) - 1 \right\} \times 1000, \qquad (6)$$

where "$X$" is $^{15}$N or $^{13}$C and "$R$" is $^{15}$N/$^{14}$N or $^{13}$C/$^{12}$C. As primary standards, pure N$_2$ and CO$_2$ gases were used, calibrated against IAEA reference standards N1, N2, N3, NBS22, and USGS24. In addition to the standard calibration at the beginning of each run, standard materials (caffeine, peptone, and acetanilide) were also included within runs to identify any drift and ensure the accuracy and full combustion of the samples during analysis. Overall analytical precision was ± 0.1‰ for $\delta^{15}$N and $\delta^{13}$C.

To determine stable carbon isotope fractionation between methane and soft tissue of cultured deep-sea mussels, two samples of the 4% methane–air mixture were taken with Tedlar® gas sampling bags. Methane was separated from other gases by gas chromatography and subsequently converted to CO$_2$ in a combustion oven, which is connected to a Thermo MAT 253 continuous-flow isotope ratio mass spectrometer (CF-IRMS, Thermo Fisher Scientific). All measured $^{13}$C/$^{12}$C ratios are given in the common delta notation as ‰-fractionation vs. the Vienna PeeDee Belemnite standard. Reproducibility of ± 0.3‰ (2 SD) is based on repeated measurements of the laboratory reference gas.

Finally, shifts of soft tissue stable isotope signatures after transplantation to a site with differently fractionated N or C can be interpreted as turnover and, therefore, as a measure of metabolic rates (Dattagupta et al. [2004]). In that sense, annual carbon turnover rates of whole *G. childressi* soft tissue were calculated as

$$\%\Delta\delta^{13}\mathrm{C}_\mathrm{ann} = \left(\delta^{13}\mathrm{C}_\mathrm{mc} - \delta^{13}\mathrm{C}_{t0}\right) / \left(\delta^{13}\mathrm{C}_\mathrm{source} - \delta^{13}\mathrm{C}_{t0}\right) \times 100 / t_c \times 12, \qquad (7)$$

where "$m_c$" are cultured mussels, "$t_0$" are the mussels sampled directly after arrival at GEOMAR and "$t_c$" represents the time (duration) of the culture [months].

### Data analyses

The dependence of seawater methane concentrations from air %CH$_4$ was analyzed by linear regression. As we could not replicate the treatments in this proof-of-concept study (all mussels of a given nutrition treatment were cultured in the same aquarium and, thus, were not independent of each other), no statistical tests were possible when analyzing *G. childressi* condition, behavior, and energy uptake data. We, hence, just described trends of averaged values of usually three individual mussels when analyzing conditions index, clearance rate and stable isotopes. Trend lines added to shell increment, valve gape activity, and gas consumption data points allowed to visualize linear, polynomial, or exponential trends in the data. The relation of cultured *G. childressi* O$_2$ consumption rate and CH$_4$ consumption rate (measured in separate respirometer vessels) was analyzed by linear regression. Differences between trends of gas consumption rates of the two different mussel batches were analyzed by adding 95% confidence envelopes.

## System performance: Results

### Performance of methane supply

With the here described system, we are able to maintain maximum seawater methane concentrations in the aquarium system at ∼60 $\mu$mol L$^{-1}$ (Fig. 4; Supporting Information Fig. S1), which corresponds well to an expected methane equilibrium concentration of the injected 4% methane in air mixture of 62.14 $\mu$mol L$^{-1}$ (using Bunsen solubility coefficient at salinity 34 and 8°C; Wiesenburg and Guinasso 1979). These values are higher than lower concentrations measured within *Gigantidas* beds in the Gulf of Mexico ("Bush Hill": 20–56 $\mu$mol L$^{-1}$ CH$_4$, "Green Canyon": 42–10,744 $\mu$mol L$^{-1}$ CH$_4$, Nix et al. 1995, Smith et al. 2000), similar to those provided by Colaço et al. (2006) to their *Bathymodiolus azoricus*
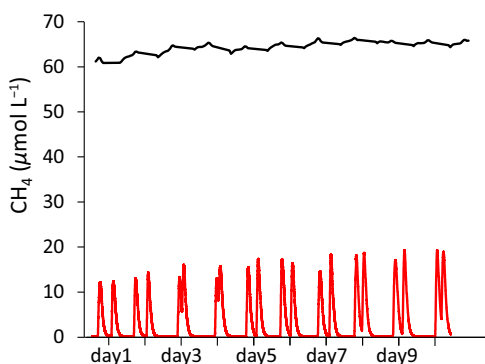


**Fig. 4.** Comparison of intermittent methane feeding by repetitive addition of 5 L of methane-saturated seawater (after 15 min of equilibration with a gas diffusor stone, solution containing ∼ 8 mmol of CH$_4$) to the 200 L recirculation culture system (red line) with continuous methane feeding by bubbling with methane-enriched air (4% methane) from the gas mixing device (black line) as measured with a CONTROS HydroC® CH$_4$ sensor in the filter tank.

culture (∼70 $\mu$mol L$^{-1}$ CH$_4$), and allowed us to culture *G. childressi* for years. Deviations from optimal (stable) CH$_4$ concentrations were caused intentionally when major improvements of the gas mixture supply (improvements of gas flow volume in the system in February 2015 and July 2017) or maximal %CH$_4$ level (July 2017) could be realized, or when experiments were conducted that had to take place in the same culture system (Supporting Information Fig. S1). During such experiments, desired CH$_4$ levels could be selected by changing the %CH$_4$ in the air–methane mixture bubbled into the system between 0% and 4% CH$_4$ (Fig. 5). More seldom (six times over the entire culture period) technical malfunctions caused reductions of methane concentrations. Overall, these intentional and non-intentional incidents together accounted for a significant amount of variation in the seawater methane concentration, most prominently so during the phase October 2017–March 2019, where the methane concentration was 57.3 $\mu$mol L$^{-1}$ ± 19.7 SD (Supporting Information Fig. S1). However, when excluding the phases of experimental work during that phase, the methane concentration was 65.7 $\mu$mol L$^{-1}$ ± 5.4 SD, demonstrating that the system is capable of maintaining very stable seawater methane concentrations.

### Mussel condition and growth

Batch 2 *G. childressi* acclimated to CH$_4$ ("m") or CH$_4$ and microalgae addition ("a + m"), maintained condition indices similar to those of the freshly imported animals ("$t_0$") even after more than 2 yr of culture (Fig. 6a). Only smaller *G. childressi* specimens of batch 1 that were cultured at less optimal CH$_4$ concentrations and batch 2 mussels that were exclusively fed with microalgae ("a", no CH$_4$) were characterized by lower condition indices. In the latter treatment, only half as many *G. childressi* survived when compared to treatments with CH$_4$ supply (Fig. 6b). Smith et al. (2000) showed that freshly collected mussels from Brine Pool NR-1 had ca. twofold higher condition indices than our batch 1 mussel from the same site (Fig. 6).

Good condition indices in batch 2 animals that received methane as an energy source ("m" and "a + m") suggest that the energy supply was sufficient to prevent consumption of body mass during the culturing experiment. The observation of a net shell thickness increase in all examined batch 1 specimens furthermore indicates that surplus energy could be invested into anabolic processes (Fig. 7). Shell thickness increased exponentially with mussel size (Fig. 7b). On the other hand, shell length increase remained low: calcein markings of 10 individual batch 1 shells revealed an increment of shell lengths between 0 to 1700 $\mu$m during the culturing period of 21 months (Fig. 7a), independently of mussel size. No shell length increments were observed in two animals. Only one mussel grew 1.7 mm in shell length, all other animals grew by 400 $\mu$m or less. No shell length growth could be detected in batch 2 animals, which were marked by shell (periostracum) scrapings, only.
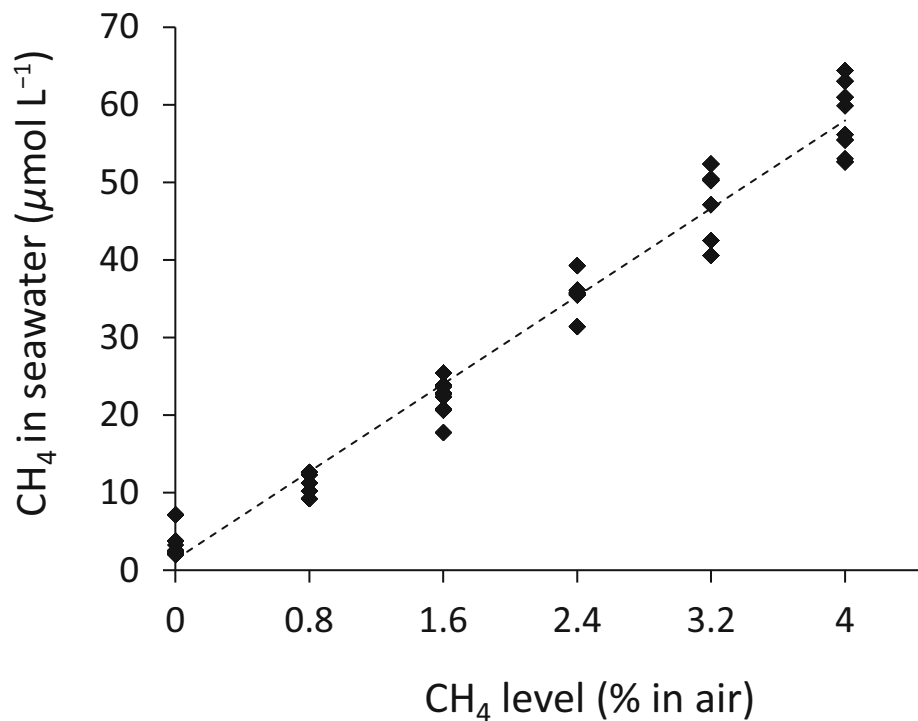
**Fig. 5.** System performance during the mussel valve gape activity experiment: Daily averages of measured $CH_4$ concentrations in the recirculating aquarium system at six different $CH_4$ concentrations (%) in the air used to equilibrate the seawater. $CH_4$ ($\mu$mol $L^{-1}$) = 14.259 %$CH_4$ + 1.5169; $R^2$ = 0.98, linear regression: $F$ = 1294.2, $p$ < 0.001; $n$ = 6.

### Methane and oxygen consumption of deep-sea mussels

Batch 1 mussels' methane consumption rates ranged between 0.03 and 0.17 $\mu$mol $g^{-1}$ $h^{-1}$, batch 1 oxygen consumption rates between 0.18 and 0.92 $\mu$mol $g^{-1}$ $h^{-1}$ (Fig. 8a). There was a slight trend toward an increasing oxygen consumption of mussels at higher methane consumption rates ($MO_2$ = 1.06 ($\pm$ 3.15, 95% CI) $MCH_4$ + 0.33 ($\pm$ 0.28, 95% CI) [$\mu$mol $g^{-1}$ $h^{-1}$]; regression: $R^2$ = 0.05, $F$ = 0.56, $p$ = 0.47; I. in Fig. 8a). Methane consumption rates of batch 2 *G. childressi* that were cultured with methane supply ("m" and "a + m") ranged between 0.1 and 0.23 $\mu$mol $g^{-1}$ $h^{-1}$ in 2017 and had increased to a range between 0.17 and 0.82 $\mu$mol $g^{-1}$ $h^{-1}$ in 2019 (Fig. 8b). In 2017, oxygen consumption of batch 2 mussels increased significantly with higher methane consumption rates: $MO_2$ = 2.19 ($\pm$ 1.78, 95% CI) $MCH_4$ + 0.54 ($\pm$ 0.24, 95% CI) [$\mu$mol $g^{-1}$ $h^{-1}$] (regression: $R^2$ = 0.55, $F$ = 8.49, $p$ = 0.023; II. in Fig. 8a).

### G. childressi *gape behavior in relation to water methane concentration*

The number of daily valve gape hours of batch 2 mussels averaged across all three repeated runs of diurnal variations of seawater $CH_4$ concentration (Supporting Information Fig. S5) was independent of the nutritional treatments the *G. childressi* were previously acclimatized to ("m": 10.7 h $d^{-1}$ $\pm$ 1.3 SD, "a + m": 11.8 h $d^{-1}$ $\pm$ 2.0 SD, "a": 11.7 h $d^{-1}$ $\pm$ 3.3 SD).

However, deep-sea mussels that were acclimatized to $CH_4$ on average reacted slightly different to changes in seawater $CH_4$ than mussels that were exclusively acclimated to microalgae food without $CH_4$ addition. Overall, we found a trend toward the longest activity phases of *G. childressi* at intermediate seawater $CH_4$ concentrations (20–45 $\mu$mol $L^{-1}$), and not at the highest concentration (57 $\mu$mol $L^{-1}$, Fig. 9). All mussels reduced valve gaping time periods in the absence of $CH_4$ in seawater. This pattern—as well as the reduced activity at the highest $CH_4$ level—was most prominent at *G. childressi* that were acclimated to $CH_4$ ("m" and "m + a"; Figs. 9a, 10b). The reactions of deep-sea mussels to changes in seawater $CH_4$ appeared to be generally stronger when $CH_4$ levels were gradually increased (Supporting Information Fig. S6a–c) as to when the $CH_4$ concentration was reduced (Supporting Information Fig. S6d–f).

### Particulate food consumption

Batch 1 *G. childressi* cleared both *Rhodomonas* sp. and *Nannochloropsis* sp. cells from seawater (Fig. 10a); however, *Rhodomonas* sp. was cleared at a higher rate. Larger mussels (shell length 77 $\pm$ 4 mm) were characterized by higher phytoplankton clearance rates than smaller mussels (shell length 51 $\pm$ 3 mm). After being cultured for 8 months under different nutritional scenarios, batch 2 *G. childressi* showed different *Rhodomonas* sp. clearance behavior: mussels acclimated to $CH_4$ and microalgae food
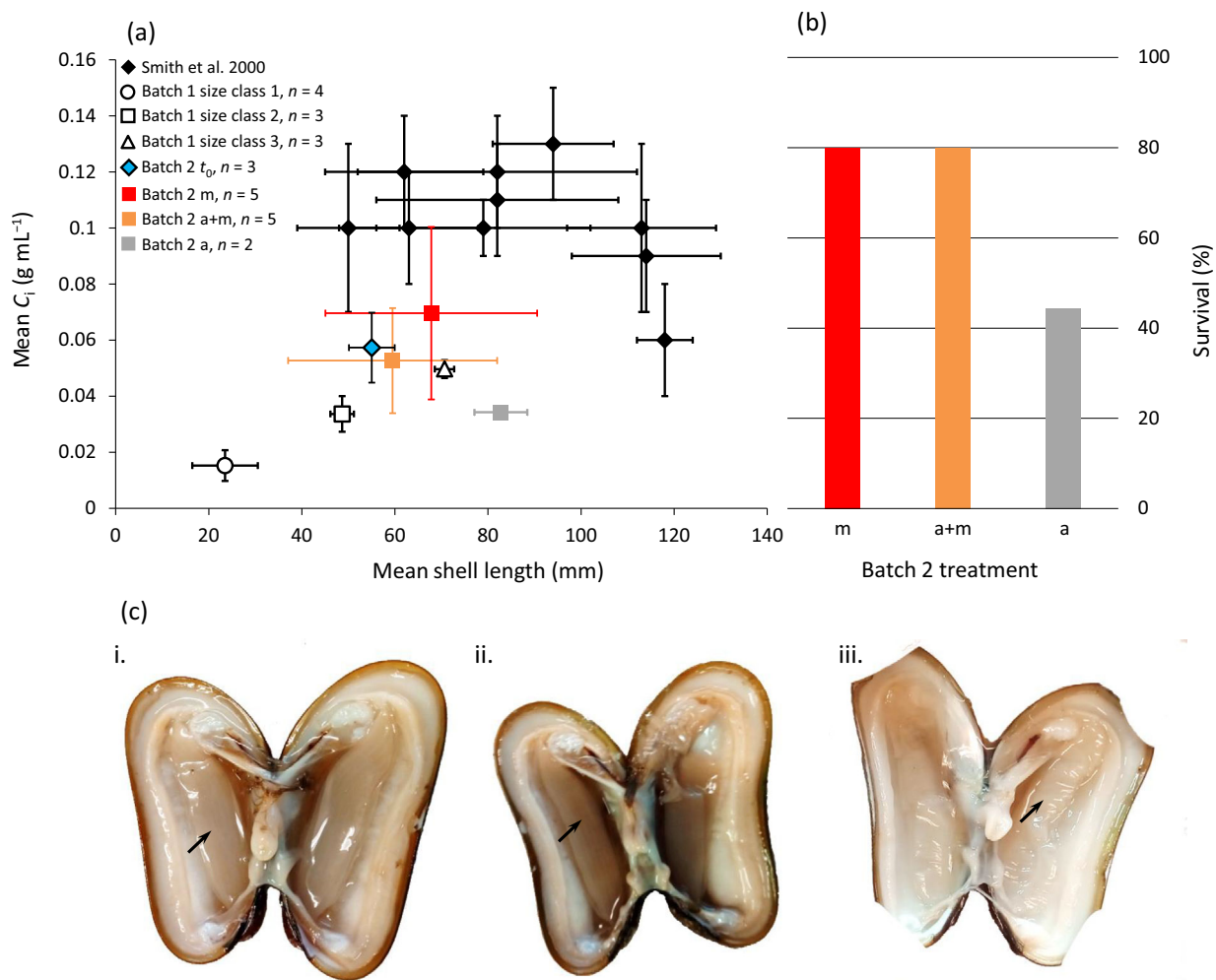
**Fig. 6.** Condition (**a**, **c**) and survival (**b**) of batch 1 and 2 *Gigantidas childressi*. (**a**) Condition of "$t_0$" mussels was determined when batch 2 mussels arrived in Kiel. *G. childressi* from batch 1 (cultured from July 2014 to August 2016) as well as from three different nutritional treatments of batch 2 (cultured from August 2017 to November 2019, "m": $CH_4$, "a + m": algae and $CH_4$, "a": algae) were sampled after 23 and 27 months of culture, respectively. Data in (**a**) are mean ± SD. (**b**) Mortality of animals in treatments "m," "a + m," and "a" that were not sacrificed for other analyses (initial animal numbers: 9–10). (**c**) Examples of freshly sacrificed batch 2 mussels from different nutritional treatments ($CH_4$: "m", algae + $CH_4$: "a + m", only algae: "a") illustrate white—almost transparent—gills (arrows) of mussels fed without methane.

supply ("a + m") cleared *Rhodomonas* at highest rates of 91.1 mL h$^{-1}$ (Fig. 10b) which corresponds to $6.4 \times 10^5$ cells h$^{-1}$ (respectively 1.12 J h$^{-1}$; at 1.75 $\mu$J cell$^{-1}$; Riisgård et al. 2012). *G. childressi* that were previously acclimated to $CH_4$-free seawater ("a") cleared *Rhodomonas* sp. in the absence of $CH_4$—but not when the seawater was enriched with $CH_4$ (Fig. 10b).

### Stable isotopes

Tissue-stable isotope signatures of the analyzed *G. childressi* ($\delta^{15}N$: −2.57‰ to 1.22‰ and $\delta^{13}C$: −59.5‰ to −54.4‰) were well in the range of those of other *G. childressi* specimens collected in the Green Canyon area in the Gulf of Mexico (MacAvoy et al. 2008; Becker et al. 2010). However, all cultured mussels had a slightly

(3‰) higher average $\delta^{13}C$ signature (−56.3‰) as compared to the mussels sampled when they arrived in Kiel (without being influenced by our artificial nutritional treatments: "$t_0$" = −59.3‰, Fig. 11b). Moreover, this difference was slightly stronger (4.5‰) in *G. childressi* that were cultured with microalgae only when compared to mussels that (also or solely) received $CH_4$ as a carbon source (2.44‰). This can be explained by the consumption of $^{13}C$-enriched *Rhodomonas* sp. microalgae (−34‰), as compared to the $\delta^{13}C$ value of $CH_4$ (−42.5‰), which was used to equilibrate the aquaria. Annual carbon turnover rates, calculated as %$\Delta\delta^{13}C_{ann}$, were 7.9% for "a"-cultured *G. childressi* and 7.6% for "m"-cultured mussels. Finally, only *G. childressi* that were acclimated to a pure microalgae diet ("a") showed a weak tendency toward a positive $\delta^{15}N$ signature (Fig. 11a).
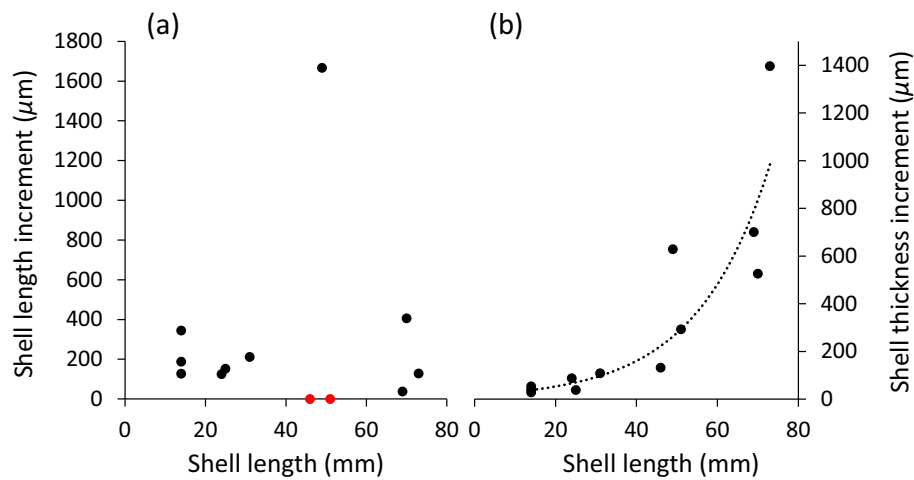
**Fig. 7.** Batch 1 *Gigantidas childressi* shell length (SL, **a**) and shell thickness (ST, **b**) growth after 21 months, as deduced from calcein staining marks using a Leica M165 FC stereo microscope. No shell length increments were observed in two animals: red dots in (**a**). Shell thickness exponentially increased with mussel size (**b**; ST increase ($\mu$m) = $17.737e^{0.055x}$, $x$ = SL (mm), $R^2$ = 0.89).
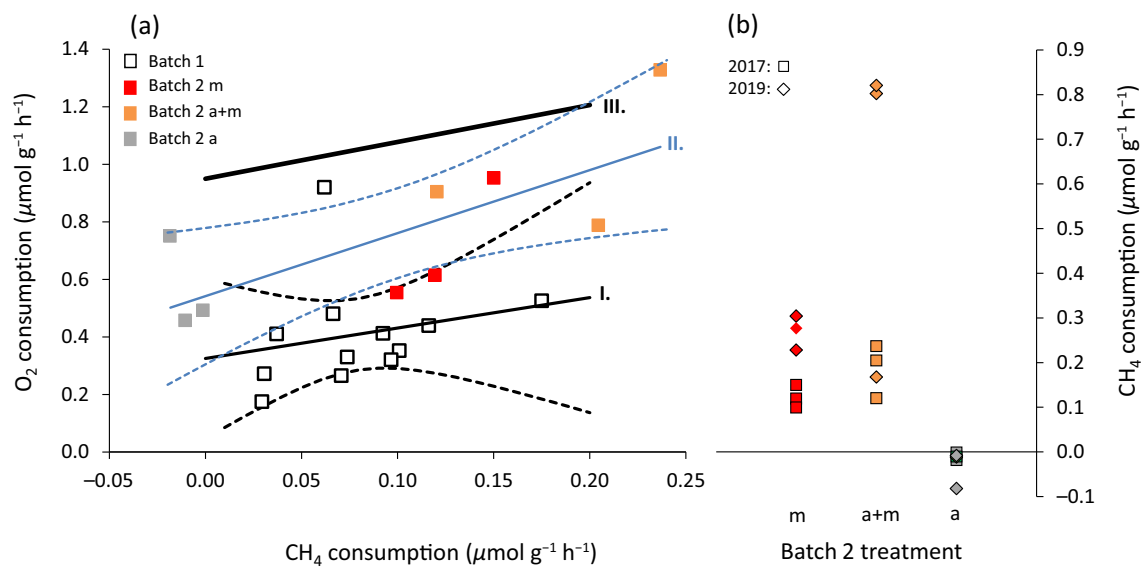


**Fig. 8.** Gas consumption of batch 1 and 2 *Gigantidas childressi*. Oxygen consumption depending on methane consumption rate (**a**) with similar average slope but overall lower oxygen uptake of cultured batch 1 animals (I.) as compared to the relationship found by Kochevar et al. (1992, III.: $MO_2$ ($\mu$mol $g^{-1}$ $h^{-1}$) = 1.19 ($\pm$ 0.09, 95% CI) $MCH_4$ ($\mu$mol $g^{-1}$ $h^{-1}$) + 0.95). Batch 2 mussels were cultured under three different nutrition regimes ($CH_4$: "m"; algae + $CH_4$: "a + m"; only algae: "a"; II.). Dashed lines in (**a**) represent 95% confidence envelopes. Methane consumption of batch 2 mussels was measured twice, in 2017 and 2019 (**b**).

The calculated annual N turnover rate (%$\Delta\delta^{15}N_{ann}$) of "a" cultured *G. childressi* was 3.9%.

## Discussion

Culture systems that allow for long-term studies of deep-sea organisms are difficult to realize and, hence, rare. Deep-sea-mussels *G. childressi* gain the majority of their energy from methanotrophic bacteria in their gills. A sufficient supply of methane is, therefore, essential for a successful culture. At

other institutes, bathymodioline mussels have been supplied with methane by repeated provision of methane-enriched sea-water, for example, by placing baskets with mussels for a limited time in a tank containing methane-saturated seawater (Arellano and Young 2009, 2011; Supporting Information Table S1). In a similar first feeding attempt, we initially supplied 5 L of methane-saturated seawater (corresponding to 8 mmol $CH_4$) into the header tank of the 200 L culture system twice a day. This treatment, however, was labor intensive and—as methane left the system quickly—resulted in hours of
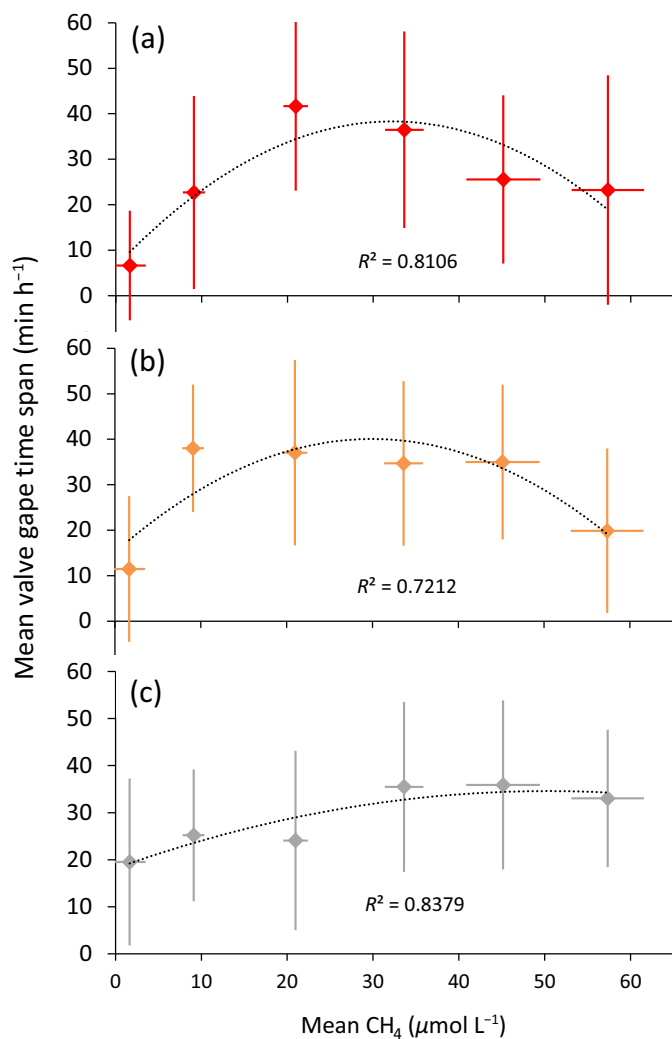
**Fig. 9.** Valve gape activity of *Gigantidas childressi* mussels from different nutritional treatments (**a**: CH$_4$ "m"; b: algae + CH$_4$ "a + m"; c: algae "a") in response to mean steps (including both, stepwise increasing and decreasing methane levels) of seawater CH$_4$ concentrations (each three times) based on time lapse image analysis. Data are mean ± SD, $n = 3$.



**Fig. 10.** Clearance rates (RC) of *Gigantidas childressi* mussels filtering phytoplankton. (**a**) RC of different-sized batch 1 mussels ("small": 51 ± 3 mm SD, "large": 77 ± 4 mm SD) that received either *Rhodomonas* or *Nannochloropsis* cells. (**b**) Clearance trials of batch 2 mussels from different nutritional treatments (CH$_4$: "m"; algae + CH$_4$: "a + m"; only algae: "a") filtering *Rhodomonas* cells. The measurement of clearance rates of *G. childressi* cultured in the "a" treatment (without CH$_4$ supply) was conducted twice: once while mussels were placed in CH$_4$-enriched seawater, and, subsequently, once without CH$_4$. Data are mean ± SE.

methane deficiency between methane peaks (Fig. 4). Under such conditions, the mussel culture could not be maintained for more than ∼ 6 months (own trials). However, a *B. azoricus* recirculating culture system at LabHorta, Azores, that was continuously equilibrated with methane (creating ∼70 $\mu$mol L$^{-1}$ of methane; no continuous methane measurements), enabled mussel survival for more than 12 months (Colaço et al. 2006). Therefore, we also developed a system with a constant—and safe—methane supply to our *G. childressi* culturing system.

Here, we present a recirculation aquarium system with an attached CH$_4$–air gas mixing device, in which we can keep deep-sea mussels (*G. childressi*) for years in good condition. We also demonstrate that variation in seawater methane concentration impacts methane and oxygen consumption rates of
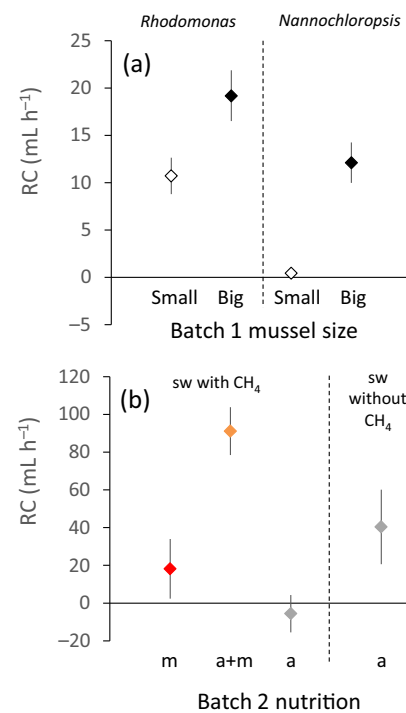
experimental animals, and we show that acclimation of animals to different nutritional treatments influences whole-animal physiological properties. These pilot experiments indicate a strong potential for our culture system to enable exciting experimental work to better understand the nutritional bioenergetics of symbiont-bearing deep-sea mussels.

Overall, we were able to design and set up a safe recirculating culture system in this proof-of-concept study to automatically supply deep-sea mussels with high methane levels for years. After overcoming technical limitations, namely suboptimal production of the methane–air gas mixture by the gas mixing device at the beginning of the culture period (batch 1 animals), stable concentrations of ∼60 $\mu$mol L$^{-1}$ methane in seawater via equilibration with 4% methane in air gas mixtures could be maintained consistently (Figs. 4, 5; Supporting Information Fig. S1). It is not possible to produce higher methane concentrations using this system design, as the lower explosion limit for methane does not allow for equilibration with gas mixtures containing more than 4.4% methane.

During the time in our culture system, *G. childressi* acquired energy, both, via their methanotrophic symbionts, which
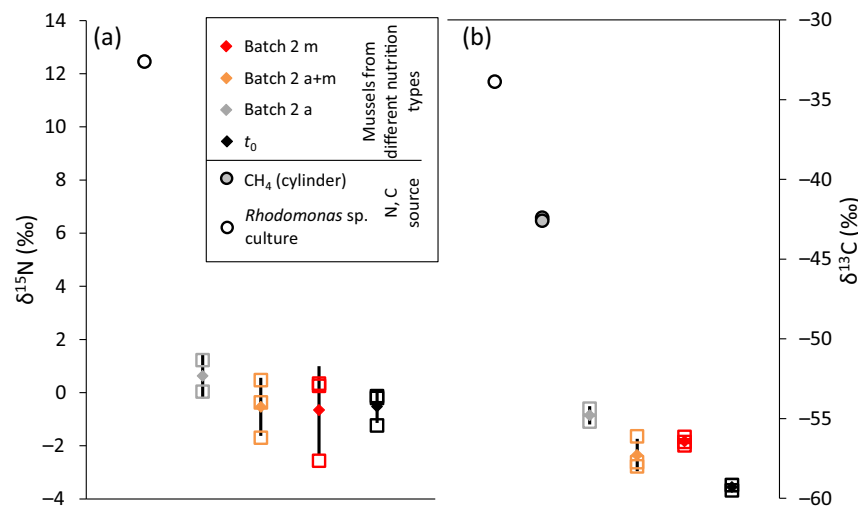
**Fig. 11.** Stable isotopes (**a**: $\delta^{15}N$, **b**: $\delta^{13}C$) of batch 2 *Gigantidas childressi* that experienced different nutritional regimes ($CH_4$: "m"; algae + $CH_4$: "a + m"; only algae: "a") in our culture. As reference, $t_0$ animals were sampled upon arrival at GEOMAR after spending 2 months post-capture at Charles Fisher's "deep-sea lab" aquarium system, Pennsylvania State University. Diamonds: mean ± SD.

oxidize the methane provided into the culture system, and from microalgae added to the seawater. Both nutritional strategies could be corroborated by direct measurements of methane and microalgae uptake. The measured maximum methane (<1 $\mu$mol $g^{-1}$ $h^{-1}$) and oxygen (<1.5 $\mu$mol $g^{-1}$ $h^{-1}$) consumption rates of *G. childressi* cultured in our system were lower than reported by Kochevar et al. (1992) (III. in Fig. 8a), who, however, had a high variance in their data and measured at much higher seawater $CH_4$ concentrations as well. Similar to those measured by Pile and Young (1999) when offering bacteria or protozoans, *G. childressi* of ~ 77mm shell length filtered microalgae more efficiently than smaller mussels. Metabolic rates appeared to be strongly reduced in batch 1 mussels, as can be seen when comparing $O_2$ consumption at similar $CH_4$ consumption rates (offset of I. and III. in Fig. 8a). Metabolic rates could be elevated by increasing $CH_4$ supply about twofold when culturing mussels of batch 2: $O_2$ and $CH_4$ consumption rates of mussels nourished with higher levels of $CH_4$ for 4.5 months (II. in Fig. 8a) were close to those measured by Kochevar et al. (1992). Furthermore, after another 2 yr of culture, the batch 2 $CH_4$ consumption rates again increased substantially (Fig. 8b), especially of those mussels that also received microalgae food ("a + m"). Lower methane consumption rates are likely due to a partial loss of methanotrophic endosymbionts in the gills during transfer from the deep sea and culture under insufficient methane supply (Kádár et al. 2005). Batches 1 and 2 animals arrived in our lab 0.5 and 2 months post-capture, respectively, and we presume that methane supply in cultures post-capture and pre-arrival to Kiel (unquantified) was suboptimal. As previous in situ work demonstrated that bathymodioline mussels can rapidly lose most

endosymbionts within weeks (Détrée et al. 2019) it is likely that this also happened before the mussels arrived in our laboratory.

The observed up to fourfold increase in methane uptake rate of batch 2 mussels may be explained by a subsequent re-acquisition of methanotrophs under our improved culture system conditions (Kádár et al. 2005; Riou et al. 2008; Tietjen et al., unpublished results). Deep-sea mussels that were fed only with microalgae apparently lost all methanotrophic symbionts, as indicated by almost transparent gills (Fig. 6c) and a lack of methane consumption after an acclimation time of 3.5 months to this regime (Fig. 8b). While these microalgae-fed animals could maintain a relatively high condition, they were characterized by a much lower survival than methane acclimated groups, indicating the ultimately unsustainable nature of this nutritional treatment. These mussels' valve gape activity was relatively unaffected by methane concentration during our behavior monitoring trials (Fig. 9). However, they filtered *Rhodomonas* sp. from the seawater only in the absence of methane, indicating a fundamental change in physiology and behavior elicited by our acclimation treatment. This was a surprising observation as the ventilation rate of *G. childressi*—unlike that of *M. edulis*—is assumed to be independent of stimuli by the filtered particles in suspension (Page et al. 1990). Also, to our knowledge, no direct methane-sensing organ has been described for deep-sea mussels so far. Valve gape activity of mussels, however, cannot be directly translated into ventilation or filtration rate, as gill-cilia driven water convection rate can be controlled independently of valve gape (Riisgård et al. 2011). On average, *G. childressi* average valve gape time for $CH_4$-supplied experimental groups increased when methane concentration was gradually increased with a maximum at intermediate values (20–45 $\mu$mol $L^{-1}$). We

assume that this preference for intermediate methane concentrations can be attributed to an increase in metabolic activity of the methanotrophic endosymbiont bacteria with rising methane concentrations and saturation of their methane requirements at high seawater methane concentrations. How the methane demand of endosymbionts and water convection rate by the mussel are coordinated and regulated is unclear and can be explored in future experiments using our culturing system.

Besides a reasonably good condition index of *G. childressi* cultured in our recirculation aquarium system, almost no shell length growth and only low shell thickness growth could be detected. In comparison, shell length increments of several mm yr$^{-1}$ have been observed in the field at a seep near the sampling station our animals originated from (GC 234; Nix et al. 1995). The methane concentrations in our cultivation system—which are still lower than measured at many cold seep sites—are unlikely to be the main reason for the lower growth rates. Nix et al. (1995) measured similar or even lower methane concentrations at sites where much higher shell-length growth rates of *G. childressi* were observed. Furthermore, *G. childressi* in our culture was in good body condition, able to invest surplus energy into shell thickness growth and, hence, not starving. Our measured methane consumption rates suggest that the mussels lost a number of their methanotrophic symbionts during the transfer from the deep sea to our culture system, though—and that these were only partially able to re-grow. A higher number of "farmed" symbionts would certainly allow experimental animals to invest more energy into shell (length) growth. Low shell growth rates could also be related to the enhanced allocation of resources to gonad development: Strong investments into gonade growth rather than shell length growth during the reproductive season are typical of shallow water mytilids (Thomas et al. 2011; Melzner et al. 2020).

While shell growth was negligible, isotope data clearly reflect the assimilation of new carbon via the consumption of microalgae cells and the consumption of farmed endosymbionts. The $\delta^{13}C$ of $-59.3‰$ of mussels sampled upon arrival at GEOMAR ("$t_0$") indicates a significant input of biogenic methane (typically $<-60‰$) at the sampling site GC249. The higher $\delta^{13}C$ signature of the cultured *G. childressi* mussels ($m_c$: "m," "a + m," and "a") can only be explained by uptake of thermogenic methane (from gas cylinders: $\delta^{13}C = -42.5‰$) and/or microalgae, though (*Rhodomonas* sp.: $\delta^{13}C = -34‰$; Brooks et al. 1987; Kennicutt et al. 1992; Becker et al. 2010). The apparent distance between mussel soft tissue $\delta^{13}C$ and the respective $\delta^{13}C$ of the two C sources (thermogenic methane and *Rhodomonas* sp., respectively) can be interpreted as incomplete soft tissue turnover (Dattagupta et al. 2004). Annual C turnover rates ($\Delta\delta^{13}C_{ann}$; calculated for "a" and "m" nutritional groups of mussels) of $< 10\%$ are significantly lower than the 40–78% Dattagupta et al. (2004) calculated for *G. childressi* which were transplanted in the field and displayed strong

shell growth—and also than the 35–53% of transplanted mussels that did not grow after transplantation. Thus, the metabolism and growth of *G. childressi* living in our deep-sea recirculation aquarium system appear to have been reduced. While post-capture loss and reduced density of symbionts during most of the culture time within our culture system may partially explain the low growth rates observed, low hydrostatic pressure might be another contributing factor. (Severe) depressurization damage to DNA and shell integrity has been described, however, predominantly for bathymodioline mussels collected from depths > 1000 m (Dixon et al. 2004; Kadar et al. 2008). Dixon et al. (2004) suggest a physiological barrier for populations from depths >1000–1500 m that prevents successful acclimation to surface pressures. For *G. childressi* that live in shallower habitats (<1000 m), Arellano and Young (2009, 2011) demonstrated that gamete release and development of viable larvae can be induced at surface pressure. These findings, in combination with our results, indicate that culturing efforts under surface pressure may be sufficient to study a range of important biological processes in *G. childressi* from relatively shallow deep-sea habitats. Studies utilizing shallow water invertebrates could demonstrate significant physiological plasticity during acclimation to pressures resembling water depths of ca. 1000 m, with changes in membrane composition ("homeoviscous adaptation") likely contributing to survival at elevated pressures (Brown et al. 2019). Thus, plastic re-organization of cellular structures might enable some marine invertebrates to acclimate to pressures in the 1–100 bar range in both directions. However, comparative growth trials of experimental *G. childressi* at ambient vs. high pressure (50–80 bar) are needed to quantify the impacts of hydrostatic pressure variation on fitness. Thus, further development of the described culture system to support long-term experiments under pressures of up to 80 bar would be needed. Furthermore, meaningful ecological studies will need multiple individual culturing systems with separate filtering and methane-sensing systems for replicated measurements and factorial experiments. Due to the relatively low costs of methane-sensing equipment, this seems a realistic option for the near future (Boulart et al. 2008; Bastviken et al. 2020; Yang et al. 2022). Alternatively, higher-cost methane sensors could be rotated between replicated methane-enriched systems (e.g., daily), as our monitoring data show relatively stable methane concentrations in our pilot system when equilibrated with our gas mixing system.

## Comments and recommendations

We have shown that our newly designed recirculating culture system is suitable for long-term maintenance experiments with cold seep *G. childressi*, at seawater methane concentrations that can be found in natural deep-sea habitats of this species. Nutritional regimes involving controlled microalgae and continuous methane addition enabled good maintenance

of body condition and some shell growth. Long-term acclimation of *G. childressi* to relatively high methane concentrations (ca. 50–60 $\mu$mol L$^{-1}$) can increase methane uptake rates of experimental animals, indicating that symbiont-depleted animals may be able to increase symbiont density again. On the other hand, we show that acclimation to a microalgae diet without the addition of methane leads to phenotypes that do not consume methane anymore, suggesting a loss of symbionts. Future culturing efforts should, therefore, utilize experimental animals that were rapidly transferred from the site of capture to the culturing system to prevent this initial loss in symbiont density and diversity.

With the caveats mentioned above in mind (potential depressurization pathologies), a number of exciting questions can be addressed with the described system if it is properly replicated. First, experimental modulation of symbiont density through seawater methane supply will enable fundamental studies related to the nutritional contributions of particulate food vs. energy and nutrients derived from the consumption of symbionts to the host mussel energy budget. Metabolic exchange processes between symbiotic partners can be studied, as well as methane-sensing processes of mussel host and symbiont and how they drive water convection activity of the host to supply methane to symbionts. Arellano and Young (2009) demonstrated the successful generation of *G. childressi* larvae in their laboratory, but were only able to rear larval stages to the first shell-forming stage. Future studies can build on this work by closely monitoring gonadal status in dependence on the availability of particulate food (Tyler et al. 2006). This can help to maintain mussels in good condition for reproduction and to spawn parental animals to raise larval stages, ideally to settlement. Such data are urgently needed to better constrain biophysical models to estimate the connectivity of deep-sea mussel populations (Breusing et al. 2016). Key parameters, such as details of larval development, swimming speed and behavior, as well as chemotactic abilities are unknown at present. Methane-sensing abilities of larvae and adults could be studied in detail (and independent of repeated collections of new mussels) using our culturing system by creating methane gradients in behavioral trials. Currently, nothing is known about the methane-sensing abilities of *G. childressi*, but it was already speculated that unknown sense organs might exist to guide larvae to seep sites once they are competent for settlement (Franke et al. 2021). Thus, we hope that culture systems as described here will stimulate more research to in detail investigate how these fascinating mussel holobionts function and how they can be protected in a deep-sea environment that is increasingly exploited.

## References

Arellano, S. M., and C. M. Young. 2009. Spawning, development, and the duration of larval life in a deep-sea cold-seep mussel. Biol. Bull. **216**: 149–162. doi:10.1086/BBLv216n2p149

Arellano, S. M., and C. M. Young. 2011. Temperature and salinity tolerances of embryos and larvae of the deep-sea mytilid mussel "*Bathymodiolus*" *childressi*. Mar. Biol. **158**: 2481–2493. doi:10.1007/s00227-011-1749-9

Bange, H. W., K. Bergmann, H. P. Hansen, A. Kock, R. Koppe, F. Malien, and C. Ostrau. 2010. Dissolved methane during hypoxic events at the Boknis Eck time series station (Eckernförde Bay, SW Baltic Sea). Biogeosciences **7**: 1279–1284. doi:10.5194/bg-7-1279-2010

Bastviken, D., J. Nygren, J. Schenk, R. Parellada Massana, and N. T. Duc. 2020. Technical note: Facilitating the use of low-cost methane (CH$_4$) sensors in flux chambers—Calibration, data processing, and an open-source make-it-yourself logger. Biogeosciences **17**: 3659–3667. doi:10.5194/bg-17-3659-2020

Becker, E. L., R. W. Lee, S. A. Macko, B. M. Faure, and C. R. Fisher. 2010. Stable carbon and nitrogen isotope compositions of hydrocarbon-seep bivalves on the Gulf of Mexico lower continental slope. Deep-Sea Res. II: Top. Stud. Oceanogr. **57**: 1957–1964. doi:10.1016/j.dsr2.2010.05.002

Berger, M. S., and C. M. Young. 2006. Physiological response of the cold-seep mussel *Bathymodiolus childressi* to acutely elevated temperature. Mar. Biol. **149**: 1397–1402. doi:10.1007/s00227-006-0310-8

Bergquist, D. C., C. Fleckenstein, J. Knisel, B. Begley, I. R. MacDonald, and C. R. Fisher. 2005. Variations in seep mussel bed communities along physical and chemical environmental gradients. Mar. Ecol. Prog. Ser. **293**: 99–108. doi:10.3354/meps293099

Bernard, B. B., J. M. Brooks, and W. M. Sackett. 1976. Natural gas seepage in the Gulf of Mexico. Earth Planet. Sci. Lett. **31**: 48–54. doi:10.1016/0012-821X(76)90095-9

Bettencourt, R., V. Costa, M. Laranjo, D. Rosa, L. Pires, A. Colaço, H. Lopes, and R. Serrão-Santos. 2011. Out of the deep sea into a land-based aquarium environment: Investigating physiological adaptations in the hydrothermal vent mussel *Bathymodiolus azoricus*. ICES J. Mar. Sci. **68**: 357–364. doi:10.1093/icesjms/fsq119

Billett, D. S. M., R. S. Lampitt, A. L. Rice, and R. F. C. Mantoura. 1983. Seasonal sedimentation of phytoplankton to the deep-sea benthos. Nature **302**: 520–522. doi:10.1038/302520a0

Boulart, C., M. C. Mowlem, D. P. Connelly, J.-P. Dutasta, and C. R. German. 2008. A novel, low-cost, high performance dissolved methane sensor for aqueous environments. Opt. Express **16**: 12607–12617. doi:10.1364/OE.16.012607

Breusing, C., and others. 2016. Biophysical and population genetic models predict the presence of "phantom" stepping stones connecting mid-Atlantic ridge vent ecosystems. Curr. Biol. **26**: 2257–2267. doi:10.1016/j.cub.2016.06.062

Brooks, J. M., M. C. Kennicutt II, C. R. Fisher, S. A. Macko, K. Cole, J. J. Childress, R. R. Bidigare, and R. D. Vetter. 1987. Deep-sea hydrocarbon seep communities: Evidence for

energy and nutritional carbon sources. Science **238**: 1138–1142. doi:10.1126/science.238.4830.1138

Brown, A., S. Thatje, A. Martinez, D. Pond, and A. Oliphant. 2019. The effect of high hydrostatic pressure acclimation on acute temperature tolerance and phospholipid fatty acid composition in the shallow-water shrimp *Palaemon varians*. J. Exp. Mar. Biol. Ecol. **514–515**: 103–109. doi:10.1016/j.jembe.2019.03.011

Cary, S. C., C. R. Fisher, and H. Felbeck. 1988. Mussel growth supported by methane as sole carbon and energy source. Science **240**: 78–80. doi:10.1126/science.240.4848.78

Childress, J. J., C. R. Fisher, J. M. Brooks, M. C. Kennicutt II, R. Bidigareand, and A. E. Anderson. 1986. A methanotrophic marine molluscan (Bivalvia, Mytilidae) symbiosis: Mussel fueled by gas. Science **233**: 1306–1308. doi:10.1126/science.233.4770.1306

Colaço, A., and others. 2006. Annual spawning of the hydrothermal vent mussel, *Bathymodiolus azoricus*, under controlled aquarium conditions at atmospheric pressure. J. Exp. Mar. Biol. Ecol. **333**: 166–171. doi:10.1016/j.jembe.2005.12.005

Cordes, E. E., D. C. Bergquist, and C. R. Fisher. 2009. Macroecology of Gulf of Mexico cold seeps. Ann. Rev. Mar. Sci. **1**: 143–168. doi:10.1146/annurev.marine.010908.163912

Coughlan, J. 1969. The estimation of filtering rate from the clearance of suspensions. Mar. Biol. **2**: 356–358. doi:10.1007/BF00355716

Dattagupta, S., D. C. Bergquist, E. B. Szalai, S. A. Macko, and C. R. Fisher. 2004. Tissue carbon, nitrogen, and sulfur stable isotope turnover in transplanted *Bathymodiolus childressi* mussels: Relation to growth and physiological condition. Limnol. Oceanogr. **49**: 1144–1151. doi:10.4319/lo.2004.49.4.1144

Dattagupta, S., J. Martin, S. M. Liao, R. S. Carney, and C. R. Fisher. 2007. Deep-sea hydrocarbon seep gastropod *Bathynerita naticoidea* responds to cues from the habitat-providing mussel *Bathymodiolus childressi*. Mar. Ecol. **28**: 193–198. doi:10.1111/j.1439-0485.2006.00130.x

Davenport, J., and X. Chen. 1987. A comparison of methods for the assessment of condition in the mussel (*Mytilus edulis* L.). J. Moll. Stud. **53**: 293–297. doi:10.1093/mollus/53.3.293

Détrée, C., I. Haddad, E. Demey-Thomas, J. Vinh, F. H. Lallier, A. Tanguy, and J. Mary. 2019. Global host molecular perturbations upon in situ loss of bacterial endosymbionts in the deep-sea mussel *Bathymodiolus azoricus* assessed using proteomics and transcriptomics. BMC Genomics **20**: 109. doi:10.1186/s12864-019-5456-0

Dixon, D. R., A. M. Pruski, and L. R. J. Dixon. 2004. The effects of hydrostatic pressure change on DNA integrity in the hydrothermal-vent mussel *Bathymodiolus azoricus*: Implications for future deep-sea mutagenicity studies. Mutat. Res. **552**: 235–246. doi:10.1016/j.mrfmmm.2004.06.026

Duperron, S., M. Sibuet, B. J. MacGregor, M. M. M. Kuypers, C. R. Fisher, and N. Dubilier. 2007. Diversity, relative abundance and metabolic potential of bacterial endosymbionts in three *Bathymodiolus* mussel species from cold seeps in the Gulf of Mexico. Environ. Microbiol. **9**: 1423–1438. doi:10.1111/j.1462-2920.2007.01259.x

Faure, B., S. W. Schaeffer, and C. R. Fisher. 2015. Species distribution and population connectivity of deep-sea mussels at hydrocarbon seeps in the Gulf of Mexico. PloS One **10**: e0118460. doi:10.1371/journal.pone.0118460

Fiala-Médioni, A., C. Métivier, A. Herry, and M. Le Pennec. 1986. Ultrastructure of the gill of hydrothermal-vent mytilid *Bathymodiolus* sp. Mar. Biol. **92**: 65–72. doi:10.1007/BF00392747

Fisher, C. R., and J. J. Childress. 1992. Organic carbon transfer from methanotrophic symbionts to the host hydrocarbon-seep mussel. Symbiosis **12**: 221–235.

Foster-Smith, R. L. 1975. The effect of concentration of suspension on the filtration rates and pseudofaecal production for *Mytilus edulis* L., *Cerastoderma edule* (L.) and *Venerupis pullastra* (Montagu). J. Exp. Mar. Biol. Ecol. **17**: 1–22. doi:10.1016/0022-0981(75)90075-1

Franke, M., B. Geier, J. U. Hammel, N. Dubilier, and N. Leisch. 2021. Coming together—Symbiont acquisition and early development in deep sea bathymodioline mussels. Proc. R. Soc. B **288**: 20211044. doi:10.1098/rspb.2021.1044

Gage, J. D. 2003. Food inputs, utilization, carbon flow and energetics, p. 313–380. *In* P. A. Tyler [ed.], Ecosystems of the world, v. **28**. Elsevier.

Gustafson, R. G., R. D. Turner, R. A. Lutz, and R. C. Vrijenhoek. 1998. A new genus and five new species of mussels from deep sea sulfide/hydrocarbon seeps in Gulf of Mexico. Malacologia **40**: 63–112.

Holcomb, M., A. L. Cohen, and D. C. McCorkle. 2013. An evaluation of staining techniques for marking daily growth in scleractinian corals. J. Exp. Mar. Biol. Ecol. **440**: 126–131. doi:10.1016/j.jembe.2012.12.003

Hourdez, S. 2018. Cardiac response of the hydrothermal vent crab *Segonzacia mesatlantica* to variable temperature and oxygen levels. Deep-Sea Res. I Oceanogr. Res. Pap. **137**: 57–65. doi:10.1016/j.dsr.2018.03.004

Huang, H., Y. Shen, Z. Yang, H. Zhao, C. Sheng, Y. Guo, and Y. Wei. 2019. A deep-sea large-volume high-pressure simulation system—Design, analysis and experimental verification. Ocean Eng. **180**: 29–39. doi:10.1016/j.oceaneng.2019.03.050

Jacobs, P., K. Troost, R. Riegman, and J. van der Mee. 2015. Length- and weight-dependent clearance rates of juvenile mussels (*Mytilus edulis*) on various planktonic prey items. Helgol. Mar. Res. **69**: 101–112. doi:10.1007/s10152-014-0419-y

Kádár, E., R. Bettencourt, V. Costa, R. S. Santos, A. Lobo-da-Cunha, and P. Dando. 2005. Experimentally induced endosymbiont loss and re-acquirement in the hydrothermal

vent bivalve *Bathymodiolus azoricus*. J. Exp. Mar. Biol. Ecol. **318**: 99–110. doi:10.1016/j.jembe.2004.12.025

Kadar, E., A. G. Checa, A. N. D. P. Oliveira, and J. P. Machado. 2008. Shell nacre ultrastructure and depressurisation dissolution in the deep-sea hydrothermal vent mussel *Bathymodiolus azoricus*. J. Comp. Physiol. B **178**: 123–130. doi:10.1007/s00360-007-0178-z

Kennicutt, M. C., II, R. A. Burke Jr., I. R. MacDonald, J. M. Brooks, G. J. Denoux, and S. A. Macko. 1992. Stable isotope partitioning in seep and vent organisms: Chemical and ecological significance. Chem. Geol. **101**: 293–310. doi:10.1016/0009-2541(92)90009-T

Kochevar, R. E., J. J. Childress, C. R. Fisher, and E. Minnich. 1992. The methane mussel: Roles of symbiont and host in the metabolic utilization of methane. Mar. Biol. **112**: 389–401. doi:10.1007/BF00356284

Koyama, S., T. Miwa, M. Horii, Y. Ishikawa, K. Horikoshi, and M. Aizawa. 2002. Pressure-stat aquarium system designed for capturing and maintaining deep-sea organisms. Deep-Sea Res. I: Oceanogr. Res. Pap. **49**: 2095–2102. doi:10.1016/S0967-0637(02)00098-5

MacAvoy, S. E., R. S. Carney, E. Morgan, and S. A. Macko. 2008. Stable isotope variation among the mussel *Bathymodiolus childressi* and associated heterotrophic fauna at four cold-seep communities in the Gulf of Mexico. J. Shellfish. Res. **27**: 147–151. doi:10.2983/0730-8000(2008)27[147:SIVATM]2.0.CO;2

MacDonald, I. R., W. R. Callender, R. A. Burke Jr., S. J. McDonald, and R. S. Carney. 1990. Fine-scale distribution of methanotrophic mussels at a Louisiana cold seep. Prog. Oceanogr. **24**: 15–24. doi:10.1016/0079-6611(90)90016-U

Martins, I., A. Colaço, P. R. Dando, I. Martins, D. Desbruyères, P.-M. Sarradin, J. C. Marques, and R. Serrão-Santos. 2008. Size-dependent variations on the nutritional pathway of *Bathymodiolus azoricus* demonstrated by a C-flux model. Ecol. Model. **217**: 59–71. doi:10.1016/j.ecolmodel.2008.05.008

McCollom, T. M., and E. L. Shock. 1997. Geochemical constraints on chemolithoautotrophic metabolism by microorganisms in seafloor hydrothermal systems. Geochim. Cosmochim. Acta **61**: 4375–4391. doi:10.1016/S0016-7037(97)00241-X

Melzner, F., B. Buchholz, F. Wolf, U. Panknin, and M. Wall. 2020. Ocean winter warming induced starvation of predator and prey. Proc. R. Soc. B **287**: 20200970. doi:10.1098/rspb.2020.0970

Mitchell, J. H., J. M. Leonard, J. Delaney, P. R. Girguis, and K. M. Scott. 2020. Hydrogen does not appear to be a major electron donor for symbiosis with the deep-sea hydrothermal vent tubeworm *Riftia pachyptila*. Environ. Microbiol. **86**: e01522-19. doi:10.1128/AEM.01522-19

Nedoncelle, K., F. Lartaud, M. de Rafelis, S. Boulila, and N. Le Bris. 2013. A new method for high-resolution bivalve growth rate studies in hydrothermal environments. Mar. Biol. **160**: 1427–1439. doi:10.1007/s00227-013-2195-7

Nishijima, M., and others. 2010. Association of thioautotrophic bacteria with deep-sea sponges. Marine Biotechnol. **12**: 253–260. doi:10.1007/s10126-009-9253-7

Nix, E. R., C. R. Fisher, J. Vodenichar, and K. M. Scott. 1995. Physiological ecology of a mussel with methanotrophic endosymbionts at three hydrocarbon seep sites in the Gulf of Mexico. Mar. Biol. **122**: 605–617. doi:10.1007/BF00350682

Page, H. M., C. R. Fisher, and J. J. Childress. 1990. Role of filter-feeding in the nutritional biology of a deep-sea mussel with methanotrophic symbionts. Mar. Biol. **104**: 251–257. doi:10.1007/BF01313266

Paull, C. K., and others. 1984. Biological communities at the Florida escarpment resemble hydrothermal vent taxa. Science **226**: 965–967. doi:10.1126/science.226.4677.965

Pile, A. J., and C. M. Young. 1999. Plankton availability and retention efficiencies of cold-seep symbiotic mussels. Limnol. Oceanogr. **44**: 1833–1839. doi:10.4319/lo.1999.44.7.1833

Ramesh, K., M. Y. Hu, J. Thomsen, M. Bleich, and F. Melzner. 2017. Mussel larvae modify calcifying fluid carbonate chemistry to promote calcification. Nat. Commun. **8**: 1709. doi:10.1038/s41467-017-01806-8

Ravaux, J., N. Léger, G. Hamel, and B. Shillito. 2019. Assessing a species thermal tolerance through a multiparameter approach: The case study of the deep-sea hydrothermal vent shrimp *Rimicaris exoculate*. Cell Stress Chaperones **24**: 647–659. doi:10.1007/s12192-019-01003-0

Renaud, S. M., L.-V. Thinh, and D. L. Parry. 1999. The gross chemical composition and fatty acid composition of 18 species of tropical Australian microalgae for possible use in mariculture. Aquaculture **170**: 147–159. doi:10.1016/S0044-8486(98)00399-8

Riisgård, H. U., P. P. Egede, and I. Barreiro Saavedra. 2011. Feeding behaviour of the mussel, *Mytilus edulis*: New observations, with a minireview of current knowledge. J. Mar. Sci. **2011**: 312459. doi:10.1155/2011/312459

Riisgård, H. U., D. Pleissner, K. Lundgren, and P. S. Larsen. 2012. Growth of mussels *Mytilus edulis* at algal (*Rhodomonas salina*) concentrations below and above saturation levels for reduced filtration rate. Mar. Biol. Res. **9**: 1005–1017. doi:10.1080/17451000.2012.742549

Riou, V., and others. 2008. Influence of $CH_4$ and $H_2S$ availability on symbiont distribution, carbon assimilation and transfer in the dual symbiotic vent mussel *Bathymodiolus azoricus*. Biogeosciences **5**: 1681–1691. doi:10.5194/bg-5-1681-2008

Riou, V., and others. 2010. Mixotrophy in the deep sea: A dual endosymbiotic hydrothermal mytilid assimilates dissolved and particulate organic matter. Mar. Ecol. Prog. Ser. **405**: 187–201. doi:10.3354/meps08515

Sanders, H. L., and R. R. Hessler. 1969. Ecology of the deep-sea benthos. Science **163**: 1419–1424. doi:10.1126/science.163.3874.1419

Sharp, J. H. 1974. Improved analysis for "particulate" organic carbon and nitrogen from seawater. Limnol. Oceanogr. **19**: 984–989. doi:10.4319/lo.1974.19.6.0984

Shillito, B., J. Ravaux, J. Sarrazin, M. Zbinden, P.-M. Sarradin, and D. Barthelemy. 2015. Long-term maintenance and public exhibition of deep-sea hydrothermal fauna: The AbyssBox project. Deep-Sea Res. II: Top. Stud. Oceanogr. **121**: 137–145. doi:10.1016/j.dsr2.2015.05.002

Sibuet, M., and K. Olu. 1998. Biogeography, biodiversity and fluid dependence of deep-sea cold-seep communities at active and passive margins. Deep-Sea Res. II: Top. Stud. Oceanogr. **45**: 517–567. doi:10.1016/S0967-0645(97)00074-X

Smith, K. 1985. Deep-sea hydrothermal vent mussels: Nutritional state and distribution at the Galapagos Rift. Ecology **66**: 1067–1080. doi:10.2307/1940566

Smith, E. B., K. M. Scott, E. R. Nix, C. Korte, and C. R. Fisher. 2000. Growth and condition of seep mussels (*Bathymodiolus childressi*) at a Gulf of Mexico brine pool. Ecology **81**: 2392–2403. doi:10.1890/0012-9658(2000)081[2392:GACOSM]2.0.CO;2

Streams, M. E., C. R. Fisher, and A. Fiala-Médioni. 1997. Methanotrophic symbiont location and fate of carbon incorporated from methane in a hydrocarbon seep mussel. Mar. Biol. **129**: 465–476. doi:10.1007/s002270050187

Thomas, Y., J. Mazurié, M. Alunno-Bruscia, C. Bacher, J.-F. Bouget, F. Gohin, S. Pouvreau, and C. Struski. 2011. Modelling spatio-temporal variability of *Mytilus edulis* (L.) growth by forcing a dynamic energy budget model with satellite-derived environmental data. J. Sea Res. **66**: 308–317. doi:10.1016/j.seares.2011.04.015

Thomsen, J., and others. 2010. Calcifying invertebrates succeed in a naturally $CO_2$-rich coastal habitat but are threatened by high levels of future acidification. Biogeosciences **7**: 3879–3891. doi:10.5194/bg-7-3879-2010

Tunnicliffe, V., S. K. Juniper, and M. Sibuet. 2003. Reducing enviroments of the deep-sea floor, p. 81–110. *In* P. A. Tyler [ed.], Ecosystems of the world, v. **28**. Elsevier.

Tyler, P., C. M. Young, E. Dolan, S. M. Arellano, S. D. Brooke, and M. Baker. 2006. Gametogenic periodicity in the chemosynthetic cold-seep mussel "*Bathymodiolus*" *childressi*. Mar. Biol. **150**: 829–840. doi:10.1007/s00227-006-0362-9

Vajedsamiei, J., F. Melzner, M. Raatz, R. Kiko, M. Khosravi, and C. Pansch. 2021. Simultaneous recording of fltration and respiration in marine organisms in response to short-term environmental variability. Limnol. Oceanogr.: Methods **19**: 196–209. doi:10.1002/lom3.10414

Walne, P. R. 1970. Studies on the food value of nineteen genera of algae to juvenile bivalves of the genera *Ostrea*, *Crassostrea*, *Mercenaria*, and *Mytilis*. Her Maj.'s Stat. Off.

Wentrup, C., A. Wendeberg, M. Schimak, C. Borowski, and N. Dubilier. 2014. Forever competent: Deep-sea bivalves are colonized by their chemosynthetic symbionts throughout their lifetime. Environ. Microbiol. **16**: 3699–3713. doi:10.1111/1462-2920.12597

Wiesenburg, D. A., and N. L. Guinasso. 1979. Equilibrium solubilities of methane, carbon monoxide, and hydrogen in water and sea water. J. Chem. Eng. Data **24**: 356–360. doi:10.1021/je60083a006

Yang, S., S. A. Svoronos, and P. Pullammanappallil. 2022. Development of inexpensive, automatic, real-time measurement system for on-line methane content and biogas flowrate. Waste Biomass Valor. **13**: 4839–4849. doi:10.1007/s12649-022-01835-5

Young, C. M., P. A. Tyler, and R. H. Emson. 1995. Embryonic pressure tolerances of bathyal and littoral echinoids from the tropical Atlantic and Pacific Oceans, p. 325–331. *In* R. H. Emson, A. B. Smith, and A. C. Campbell [eds.], Echinoderms research 1995. Balkema.

*Submitted 16 June 2022*
*Revised 12 March 2024*
*Accepted 20 March 2024*

*Associate editor: Michael Beman*